Non-communicable inflammatory skin diseases comprise clinically meaningful distinct endotypes as identified by non-hypothesized integration of phenotypic and transcriptome data

Natalie Garzorz-Stark, MD, PhD, Christina Hillig, PhD, Heydar Maboudi Afkham, PhD, Martin Meinel, MSc, Manja Jargosch, PhD, Peter Seiringer, MD, PhD, Felix Lauffer, MD, PhD, Anna C. Pilz, MD, Xixi Li, PhD, Jigyansa Mishra, MSc, Matthias Hübenthal, PhD, Stephan Weidinger, MD, Benjamin Klein, MD, Lam C. Tsoi, PhD, Johann Gudjonsson, MD, PhD, Curdin Conrad, MD, Michel Gilliet, MD, Kenji Kabashima, MD, PhD, Fabian Theis, PhD, Carsten B. Schmidt-Weber, PhD, Tilo Biedermann, MD, Michael P. Menden, PhD, Stefanie Eyerich, PhD, Kilian Eyerich, MD, PhD

PII: S0091-6749(26)00626-3

DOI: https://doi.org/10.1016/j.jaci.2026.08.017

Reference: YMAI 17306

To appear in: *The Journal of Allergy and Clinical Immunology*

Received Date: 16 April 2026

Revised Date: 4 August 2026

Accepted Date: 9 August 2026

Please cite this article as: Garzorz-Stark N, Hillig C, Afkham HM, Meinel M, Jargosch M, Seiringer P, Lauffer F, Pilz AC, Li X, Mishra J, Hübenthal M, Weidinger S, Klein B, Tsoi LC, Gudjonsson J, Conrad C, Gilliet M, Kabashima K, Theis F, Schmidt-Weber CB, Biedermann T, Menden MP, Eyerich S, Eyerich K, Non-communicable inflammatory skin diseases comprise clinically meaningful distinct endotypes as identified by non-hypothesized integration of phenotypic and transcriptome data, *The Journal of Allergy and Clinical Immunology* (2026), doi: https://doi.org/10.1016/j.jaci.2026.08.017.

Non-communicable inflammatory skin diseases comprise clinically meaningful distinct endotypes as identified by non-hypothesized integration of phenotypic and transcriptome data

Authors: Natalie Garzorz-Stark, MD, PhD [1,2,3,*,†], Christina Hillig, PhD [4,5,†], Heydar Maboudi Afkham, PhD[1, †], Martin Meinel, MSc [4,6], Manja Jargosch, PhD[3,7], Peter Seiringer, MD, PhD[3], Felix Lauffer, MD, PhD[8], Anna C Pilz, MD[1], Xixi Li, PhD[9], Jigyansa Mishra MSc[4,5], Matthias Hübenthal, PhD[10], Stephan Weidinger, MD[10], Benjamin Klein, MD[11], Lam C Tsoi, PhD[11], Johann Gudjonsson, MD, PhD[11], Curdin Conrad, MD[12], Michel Gilliet, MD[12], Kenji Kabashima, MD, PhD[13], Fabian Theis, PhD[4,5], Carsten B. Schmidt-Weber, PhD[7,14], Tilo Biedermann, MD[3], Michael P. Menden, PhD [4,9,*,†], Stefanie Eyerich, PhD [1,7,15,†], Kilian Eyerich, MD, PhD[1,2,†]

Affiliations:

[1] Department of Dermatology and Venereology, Medical Center - University of Freiburg, Faculty of Medicine, University of Freiburg, Freiburg, Germany

[2] Division of Dermatology and Venereology, Department of Medicine Solna, and Center for Molecular Medicine, Karolinska Institutet, Stockholm, Sweden

[3] Department of Dermatology and Allergy, Technical University of Munich, Munich, Germany

[4] Computational Health Center, Helmholtz Munich, Neuherberg, Germany

[5] Department of Mathematics, Technical University of Munich, Munich, Germany

[6] Department of Biology, Ludwig-Maximilians University Munich, Martinsried, Germany

[7] ZAUM – Center of Allergy and Environment, Technical University of Munich, School of Medicine and Health & Helmholtz Munich, German Research Center for Environmental Health, Munich, Germany

[8] Department of Dermatology and Venereology, Ludwig Maximilians University Munich, Munich, Germany

[9] Department of Biochemistry & Pharmacology, Bio21 Molecular Science and Biotechnology Institute, The University of Melbourne, Parkville, Australia

[10] Department of Dermatology and Allergy, University Hospital Schleswig-Holstein, Kiel, Germany.

[11] Department of Dermatology, Michigan Medicine, University of Michigan, Ann Arbor, Michigan

[12] Department of Dermatology, Lausanne University Hospital CHUV and University of Lausanne, Lausanne, Switzerland

[13] Department of Dermatology, Graduate School of Medicine, Kyoto University, Kyoto, Japan; Singapore Immunology Network (SIgN) and Institute of Medical Biology (IMB), Agency for Science, Technology and Research (A*STAR), Biopolis, Singapore.

[14] German Center of Lung Research (DZL), Neuherberg, Germany

[15] Institute for Immunodeficiency, Center for Chronic Immunodeficiency, Medical Center-University of Freiburg, Faculty of Medicine, University of Freiburg; Freiburg, Germany

[†] these authors contributed equally to this work

*Corresponding authors:

Natalie Garzorz-Stark, MD, Ph.D., Department of Dermatology and Venereology, University of Freiburg, Hauptstraße 7, 79104 Freiburg, Germany, natalie.garzorz-stark@uniklinik-freiburg.de, phone: +49 0761 270 67160

Michael P. Menden, Ph.D., Department of Biochemistry and Pharmacology, Bio21 Molecular Science and Biotechnology Institute, The University of Melbourne, Grattan Street, Parkville, Victoria 3010, Australia, michael.menden@unimelb.edu.au, phone: +61 38344 2220

Funding

This work is supported by Deutsche Forschungsgemeinschaft (DFG) through TUM International Graduate School of Science and Engineering (IGSSE) and an ERC grant (IMCIS, 676858).

Conflict of Interests

The authors declare no competing interests related to this work.

3431 words

Abstract:

Background: Non-communicable inflammatory skin diseases (ncISDs) comprise over 100 conditions with overlapping clinical features. Current classification systems are largely based on morphology and do not adequately reflect underlying molecular mechanisms, limiting the implementation of precision therapies.

Objective: To establish a data-driven, molecular framework for stratifying ncISDs independent of conventional diagnostic categories.

Methods: We integrated 727 skin transcriptomes with clinical metadata from 390 patients across 22 ncISDs and applied unsupervised and machine-learning approaches to identify molecular endotypes and develop a predictive classifier.

Results: We identified thirteen distinct molecular endotypes, which segregated into two major groups: seven driven by immune response programs and six by metabolic and epidermal structural pathways. Common diseases such as psoriasis and eczema distributed across multiple endotypes, highlighting substantial molecular heterogeneity. Psoriasis-dominated endotypes showed differential responses to IL-23-, IL-17-, and TNF-targeted therapies, underscoring clinical relevance. A multi-endotype classifier achieved 81.4% accuracy and was validated in independent cohorts.

Conclusion: These findings define a molecularly informed framework for disease stratification that transcends traditional diagnostic boundaries and enables more precise, mechanism-based therapeutic decision-making across inflammatory diseases.

Key Messages:

- Non-communicable inflammatory skin diseases segregate into 13 molecular endotypes that transcend traditional diagnoses and reveal shared biology across clinically distinct conditions.
- Endotypes cluster into immune-driven and metabolic/epidermal structural programs, identifying a previously unrecognized disease axis beyond classical immune classifications.
- Differences in therapeutic response across endotypes were observed, suggesting that molecular classification may help inform treatment selection.

Capsule Summary

Molecular endotyping of inflammatory skin diseases reveals biologically distinct subgroups that transcend clinical diagnoses and predict therapeutic response. Our proposed framework enables precision treatment selection and redefines disease classification beyond morphology for improved patient care.

Key words

Non-communicable inflammatory skin diseases, endotypes, precision dermatology, disease heterogeneity, transcriptomics, molecular classification

Abbreviations

ncISD - Non-communicable inflammatory skin diseases
LS - Lesional skin
NL - Non-lesional skin
UMAP - Uniform Manifold Approximation and Projection
CIFG - Cluster-Informative Featured Genes
HVG - Highly variable genes

KNN - k-nearest neighbors

SVM / SVC - Support vector machine / support vector classifier

ARI - Adjusted Rank Index

PGA - Physician Global Assessment

PASI - Psoriasis Area and Severity Index

DLQI - Dermatology Life Quality Index

SCORAD - Scoring Atopic Dermatitis

RNA-seq - RNA sequencing

logCPM - Log counts per million

GEO - Gene Expression Omnibus

TNF - Tumor necrosis factor

IL - Interleukin

IL-17 / IL-23 - Interleukin-17 / Interleukin-23

Th - T helper (cell)

Treg - Regulatory T cell

IFN-γ - Interferon gamma

TGF-β - Transforming growth factor beta

G-CSF - Granulocyte colony-stimulating factor

OR - Odds ratio

Introduction

Precision medicine has transformed oncology by linking molecular alterations to targeted therapies[1, 2], yet inflammatory diseases remain classified largely by clinical phenotype despite growing therapeutic complexity. This limitation is particularly evident in dermatology, where disease ontology has historically been based on morphology[3].

Although pragmatic, phenotype-based classification often groups biologically distinct entities and does not adequately explain inter-patient heterogeneity in treatment response. As a result, many patients with inflammatory skin diseases are still managed by trial and error, with delayed disease control, unnecessary exposure to ineffective therapies, and increased healthcare burden[4]. Non-communicable inflammatory skin diseases (ncISDs) are especially suitable for a precision-medicine approach because they are common (skin conditions collectively account for 1.79% of the global disease burden[5]), clinically heterogeneous, and increasingly treatable with targeted therapies[6]. Collectively, skin conditions account for a substantial global disease burden, yet for most ncISDs no disease-specific targeted therapy is approved or in development. Even in common diseases such as psoriasis or atopic dermatitis therapeutic response remains difficult to predict. Moreover, overlapping phenotypes, including eczematized psoriasis[7] and nummular eczema[8], further complicate diagnosis and treatment selection.

Emerging stratified-medicine concepts for ncISD[9-12] posit that these disorders are primarily driven by interactions between lymphocytes and epithelial cells. Within this conceptual framework, Gilliet and colleagues recently introduced a module-based taxonomy derived from cross-comparison of transcriptomic profiles across major inflammatory skin diseases[13]. However, this approach is still hypothesis-driven and tied to traditional diagnostic labels, which can mask important molecular differences between individual patients and limits classification to broad disease clusters. We further proposed the concept of immune response patterns grouping essentially all relevant ncISD according to the underlying deviation of immune pathways into five main patterns: type 1 immunity-pattern driven by cytotoxic T cells, IFN-γ

and TNF (1), type 2 immunity-pattern mediated by Th2 cells and mediators such as IL-4 and IgE (2), type 3- immunity-pattern dominated by Th17 cells and the IL-17/IL-23 axis (3), granulomatous and fibrogenic responses characterized by Tregs and TGF-ß signaling (4) and autoinflammatory innate immune activation characterized by myeloid cells, IL-1 and TNF (5)[10, 14]. Most of these immune modules or patterns can be therapeutically targeted across entire disease clusters rather than solely within the lead indication for which drug approval was obtained[10, 11, 14]. Despite this progress, 15 to 50% of patients with ncISD, fail to respond adequately to therapy, both within approved indications and across diseases sharing similar immunopathogenic patterns.

To achieve meaningful progress toward precision medicine in inflammatory skin diseases, we propose that the conventional, symptom-based disease ontology must be complemented by molecular analysis.

Here, we introduce a hypothesis-free molecularly informed classification framework that defines disease endotypes through the systematic integration of clinical phenotyping with multi-dimensional molecular analyses. This endotype based approach transcends the traditional diagnostic boundaries, offering a mechanistic foundation for patient stratification, therapeutic guidance, and biomarker discovery across the spectrum of inflammatory skin diseases.

Methods

Study cohort

A cohort of 390 patients with non-communicable inflammatory skin diseases (ncISD) was established (“Germany South”), including a broad spectrum of inflammatory and related dermatological conditions. Diagnoses were assigned by dermatologists based on clinical presentation, histopathology, and patient history. Subdiagnoses, including eczema, psoriasis, and lupus subtypes, are listed in Table 1; In particular the eczema category included both

classical atopic dermatitis and additional eczematous phenotypes, reflecting the diagnostic heterogeneity encountered in routine clinical practice. Mycosis fungoides cases were exclusively patch stage IA with one exception of a patient in stage IVA, biologic-associated cutaneous adverse events comprised psoriasis-, eczema-, and lupus-like reactions that developed during biologic treatment for non-dermatologic conditions, primarily inflammatory bowel disease.Patients had not received systemic therapy prior to sampling. Cohort characteristics are provided in Table 1. The study was approved by the local ethics committee (Klinikum Rechts der Isar, 44/16 S), and all participants provided written informed consent. For validation, three independent cohorts were analyzed, including one unpublished German cohort ("Germany North") and two publicly available U.S. cohorts. Cohort details are summarized in Table S7.

Clinical attributes

Collection: For each patient, diagnosis, sub diagnosis, immune-response pattern assignment, and disease severity scores (PASI, SCORAD, PGA, DLQI) were recorded. In addition, a comprehensive set of in total 86 clinical, histological, laboratory, and comorbidity-related attributes was collected (Table S1). Clinical variables were categorized as nominal, ordinal, or continuous and subsequently encoded, scaled, and imputed to account for missing values. Preprocessing steps are described in detail in the Supplementary Methods.

Enrichment of attributes in endotypes: To identify attributes associated with specific endotypes, variables with excessive missingness or low variance were excluded. Enrichment was assessed using non-parametric statistical tests appropriate to the data type, and multiple testing was controlled using a predefined significance threshold.

Effect sizes for continuous, ordinal, and nominal variables were calculated using established metrics, as detailed in the Supplementary Methods.

206

207 ***Bulk RNA sequencing***

208 Lesional (LS) and non-lesional (NL) skin samples were obtained from a total of 390 patients.
209 RNA was extracted and subjected to bulk RNA sequencing. Data preprocessing, normalization,
210 and quality control were performed using standard pipelines and are described in the
211 Supplementary Methods including accession numbers for all datasets.

212

213 ***Identification of Endotypes***

214 To overcome limitations of existing unsupervised gene selection methods (e.g., dispersion-
215 based approaches, expression standard deviation) [15, 16], which are sensitive to noise in gene
216 expression measurements, we developed an unsupervised gene ranking strategy that identifies
217 highly variable genes most informative for clustering, thereby facilitating the delineation of
218 meaningful endotypes.

219 *1. Cluster-Informative Featured Genes (CIFG)*

220 Unsupervised clustering of high-dimensional data depends on feature selection. We developed
221 "Cluster-Informative Featured Genes (CIFG)" as a pre-clustering step (Figure 2B, Figure S2A–
222 M), ranking genes by their ability to partition samples without prior labels.

223 (a) Gene profiles: For each gene, normalized expression values (mean-centered) were
224 sorted across samples to capture distribution patterns and group-separating potential
225 (Figure S2J–K).

226 (b) Gene profiles were clustered using k-means (k = 50). Clusters were ranked by mean
227 expression standard deviation, and genes from higher-ranked clusters were prioritized
228 as more informative (Figure 2B; Figure S2).

229

230 *2. Clustering Methodology*

Clustering quality was assessed using the pattern-score, defined as the proportion of samples matching the dominant ground truth label within each cluster. Leiden clustering[17] was applied to a precomputed KNN graph, with resolution controlling cluster granularity.

3. Implementation and Benchmarking

CIFG was applied to 282 samples (patterns 1, 2, 3a, 5). Gene subsets (0.5%, 1%, then 2–100%) were evaluated using Leiden clustering (resolution 0.5–1.5). Expression was normalized to logCPM (edgeR) and scaled (Scikit-learn)[18]. KNN graphs (k = 1) enabled future sample assignment without re-clustering. Pattern-scores were averaged across seeds, and the Davies–Bouldin index[19] assessed cluster quality. The optimal subset (7% of genes) achieved the highest pattern-score (72.22%) and lowest Davies–Bouldin index (Figure S2G–H). These genes were used for Leiden clustering of 342 lesional samples (resolution 0.9), yielding 13 endotypes (Figure 2E). CIFG outperformed dispersion-based[16] (SCANPY20) and standard deviation methods, producing more homogeneous clusters (Figure S2N–S), confirmed by one-sided Wilcoxon tests (SciPy).

Results

Traditional disease ontology and immune-response patterns fall short in predicting treatment outcomes in ncISD

To develop a molecular classification for ncISD independent of current disease labels, a large, diverse cohort and unbiased methods resolving individual heterogeneity are required. The framework must capture molecular signatures that enable precise stratification and identification of biological drivers of clinical variation and therapy response.

Therefore, we established a cohort of 390 patients with 22 ncISDs spanning major immune response patterns[10, 12, 13]: cytotoxic (1), eczematous (2a), bullous (2b), psoriatic (3),

granulomatous/fibrogenic (4), and autoinflammatory (5) (Figure 1A, Table 1). We generated transcriptomes from lesional and/or non-lesional skin (n = 727) and profiled 86 clinical and molecular attributes, including therapy response, to derive hjghly granular individualized "phenomic fingerprints" for each patient (Figure 1B, Table S1).

UMAP of transcriptomes showed clustering by diagnosis and immune patterns (Figures 1C–D, Figure S1A-B), but many patients did not cluster with their respective disease or immune response patterns. For visualization purposes, related subdiagnoses were grouped under broader diagnostic categories in Figure 1A, whereas detailed subtype annotations are provided in Figure S1C and S1D). This observation is consistent with our systematic synthesis of published clinical evidence on pathway-targeted therapies, which shows that while some targets are highly effective within their canonical immune response patterns, others exhibit moderate, absent, or even negative effects in subsets of diseases sharing the same pattern (Figure S1E, Table S2). Together, these findings highlight the limitations of diagnosis- and pattern-based stratification approaches.

To elucidate the potential of phenomic fingerprints to dissect the heterogeneity of our patient cohort, we applied UMAP to visualize all 390 ncISD patients based on their phenomic fingerprints derived from the 86 attributes (Figure 1E). This analysis uncovered patients with similar and different phenomic fingerprints, respectively, suggesting that such individuals may exhibit similar and dissimilar responses to specific targeted therapies, respectively. However, even neighboring patients with similar clinical fingerprints and identical diagnoses may respond differently to a given therapy, while patients with dissimilar fingerprints may respond equally well to the same therapy. This is illustrated in Figure 1F using the example of psoriasis and pustular psoriasis patients, respectively, treated for 20 weeks with an interleukin (IL)-17 inhibitor. This finding was not restricted to the example patients shown (Figure 1F). Across all psoriasis patients with available therapy response data, responders and non-responders to TNF-, IL-17-, and IL-23-targeted therapies did not form distinct clusters based on their phenomic

fingerprints (Figure S1F, Interactive Supplementary Data). These results underline the need for the description of new endotypes in ncISD allowing optimal and personalized treatment regimens.

Newly defined endotypes in ncISDs identified by cluster-informative featured genes

Given the heterogeneity of ncISDs, we sought to identify biologically meaningful endotypes through clustering of normalized gene expression profiles, independent of diagnoses, patterns and clinical attributes. Because standard highly variable gene- (HVG) selection methods often capture technical rather than biologically discriminative variation, we developed CIFG, an unsupervised approach that ranks genes according to their ability to support informative clustering. CIFG outperformed dispersion- and standard deviation-based gene-selection approaches by generating more homogeneous and biologically coherent clusters while requiring fewer genes (Figure 2A-D, Figure S2A-M, Supplemental Methods). Immune-response patterns 1, 2a, 3, and 5, encompassing the majority of samples, were used to guide endotype identification (Figure 2A). Genes were ranked using CIFG (Figure 2B), and the optimal subset size was determined by cross-validation and Leiden clustering across progressively varied gene subsets (Figure 2C). Ultimately, the top 7% of CIFG-ranked genes, achieving a mean pattern score of 72.22 across folds, were selected to define the endotypes (Figure 2D). CIFG required fewer genes and yielded more homogenous and biological coherent clusters than standard methods (HVG: x = 86%, std: x = 74%, Figure S2N-S). These endotypes showed only partial concordance with traditional diagnoses and immune-response patterns, resulting in substantial reassignment of individual patients. Psoriasis, for example, was distributed across nearly all endotypes except E2 and E4, demonstrating marked molecular heterogeneity within a clinically well-defined disease. Conversely, clinically distinct diseases, including eczema, granuloma annulare, pyoderma gangrenosum, and cutaneous lymphoma, converged in shared endotypes, suggesting common pathogenic programs and potential for

cross-indication therapeutic efficacy across conventional diagnostic boundaries (Figure 2E–F, Table S3). Specifically, the Adjusted Rand Index (ARI) quantifying the concordance between classification systems indicated low to moderate concordance between traditional diagnoses and endotypes (ARI = 0.177) and between immune-response patterns and endotypes (ARI = 0.155). Notably, the 13 identified endotypes explained markedly more variance in lesional skin transcriptomes than either traditional diagnosis or immune response pattern (11.55 ± 10.57 for endotypes, 4.95 ± 7.68 for diagnoses, and 1.85 ± 4.43 for immune response patterns). Effect sizes further supported this improvement, with Cohens' d values of 0.71 for endotypes versus diagnoses (medium effect), 1.20 for endotypes versus patterns (strong effect), and 0.50 for patterns versus diagnoses (low effect, Figure 2G).

ncISD endotypes are split into immunity and metabolism-structural impairment branches and driven by distinct biological processes

Hierarchical analysis of the 13 endotypes uncovered a previously unrecognized organizing principle of ncISDs (Figure 3) indicating that shared clinical diagnoses can arise from fundamentally distinct biological programs. Endotypes separated into two major branches: one (E1-E4, E11-13) dominated by immune activation and another (E5-E10) characterized by metabolic and epidermal structural programs (Figure 3A). While immune-driven stratification is expected in inflammatory diseases, the emergence of lipid metabolism, keratinocyte differentiation, and barrier-related biology as a major independent axis was unexpected and suggests that tissue-intrinsic programs define coherent disease subgroups beyond overt inflammation. The inflammatory arm showed strong induction of immune pathways, including interleukin and G-CSF signaling, whereas the metabolic/structural arm was defined by lipid-related pathways essential for barrier function and keratinocyte differentiation (Figure 3A, B, Figure S3A).

Within the inflammatory arm, endotypes E11–E13 (predominantly psoriasis) were characterized by high expression of psoriasis-associated markers (e.g., *S100A7*, *SERPINB4*[20, 21]) and pathways related to IL-36 signaling, antimicrobial peptides, and neutrophil degranulation (Figure 3C, S3B). In contrast, endotypes E1–E4 (autoinflammatory conditions and interface dermatitis) showed upregulation of *CXCL9*, a IFNγ-induced chemokine central to interface dermatitis [22], and *FN1* encoding fibronectin, a glycoprotein involved in cell adhesion and extracellular matrix remodeling[23]. E1 and E2 separated from E3 and E4 by strong innate immune activation (*CXCL8*, *IL1B*, *IL6*), matrix metalloproteinases, and tissue-remodeling pathways (Figure 3D, S3C). Notably, E1 included a substantial proportion of eczema patients, indicating that a subset is driven by neutrophil-associated inflammation. The close relationship between E1 and E2 suggests a shared axis of tissue-destructive inflammation and stromal remodeling. Consistently, E2 showed increased fibroblasts and endothelial cells in cell type deconvolution of our bulk RNA-seq dataset, supporting a role for mesenchymal and vascular components (Figure S4).

Endotypes E3 and E4 were mainly composed of cutaneous lupus and lichen planus. Both share features of interface dermatitis, including T cell enrichment (Figure S4), upregulation of *CXCL9, IFNG*, and cell-death–associated molecules (*CARD9, CARD11*, caspases [24, 25]) (Figure 3D, Figure S3C). Despite this overlap, they segregate into distinct molecular endotypes, indicating divergent immune programs. While both show antigen presentation, E3 (mainly lichen planus) exhibits stronger type 2/3 signatures (*CCL22, IL13, S100A7A*), whereas E4 (mainly lupus) shows activation of inflammasome and type 1 signaling.

In contrast, the metabolic/structural arm (E5–E10) was enriched in eczema, which was present across all endotypes except E4 (3–71%), highlighting its clinically known heterogeneity influenced by structural impairment, immunity, ethnicity, and age[26, 27]. This branch was defined by altered fatty acid metabolism, with an initial split between E5/E6 and E7–E10 (Figure 3A, Figure S3D). E5 and E6 showed enrichment of cholesterol biosynthesis and lipid mediator

pathways (Figure 3A), including Pityriasis rubra pilaris[28] (E5) and Darier's disease (E6) [29]. In contrast, E7–E10 were linked to monoclonal T cell disorders such as cutaneous T cell lymphoma, with transcription factors RUNX2[30] and TCF4 implicated[31] in tumor initiation and progression. Overall, this hierarchy defines a molecular axis from inflammatory to metabolic/structural programs, reorganizing ncISDs into biologically coherent groups and supporting precision-medicine-based classification.

Molecular endotypes reveal clinically-relevant stratification and predict therapy response in psoriasis

To assess whether our molecular classification provides information beyond conventional diagnosis, we constructed endotype-specific networks integrating pathways, key pathway genes, transcription factor targets, and phenotypic attributes (Figure 4, Figures S5–S6). We used psoriasis as a proof-of-concept benchmark, as it is well characterized, broadly treatable with targeted therapies [32] and supported by publicly available datasets enabling validation of endotype-associated therapeutic responses, . However, predictive biomarkers are still lacking [33, 34] (Figure 4) and, leaving treatment selection largely empirical.

Psoriasis patients were mainly assigned to inflammation-driven endotypes E11–E13, but also to E5 within the metabolic/structural arm. To determine whether molecular endotypes reflected clinical subtype classification, we examined the distribution of psoriasis subtypes across the psoriasis-associated endotypes. Plaque psoriasis and the remaining clinical subtypes were distributed across multiple endotypes, indicating that endotype assignment cannot be explained by clinical subtype alone (Figure S7). E5 was enriched for acute psoriasis and clinical features such as "erythema" and "exanthema", with molecular signatures of innate immune activation and lipid metabolism (Figure 4A, Figure S5). In contrast, E11–E13 showed strong keratinization programs and classical histopathological features such as parakeratosis and dilated capillaries. We next tested whether these differences relate to therapy response. First, a

focused analysis of psoriasis patients with available therapy response was performed and further revealed differences in clinical, histopathological, and laboratory attributes across endotypes E11–E13 despite their similar clinical subtype composition (Figure S7, Figure S8). Analysis of TNF-, IL-17-, and IL-23–targeted treatments (PGA/PASI at week 12; Table S4) revealed distinct endotype-specific responses. IL-17 inhibition was more effective in E11 and E13 than E12, whereas IL-23 inhibition showed the highest responses in E12 compared with E5, E11, and E13 (Figure 4B). Consistently, IL-23 signaling and *NOS2* expression were strongest in E12, while keratinization pathways dominated E11 and E13.

Together, these findings show that psoriasis comprises molecularly distinct endotypes with different biological drivers and therapy responses. Collectively, this analysis illustrates that molecular endotyping of ncISDs captures clinically actionable biological heterogeneity not apparent from conventional diagnosis alone and highlights the potential of this framework to support mechanism-based therapeutic stratification.

Molecular classifiers for clinical translation of ncISD endotypes

Clinical translation of ncISD endotypes requires robust molecular classifiers that predict patient endotypes with high confidence using a limited number of markers. We therefore developed a linear SVM classifier, achieving 81.4% ± 7.5% accuracy with 131 genes, far exceeding random assignment of 8% ± 3% accuracy (Figure 5A, B). Performance remained strong with a reduced 25-gene signature (73.5% ± 9.5%, Figure S9). Top-ranked genes mapped to core endotype programs, supporting biological coherence (Figure 4, Figure 5C, Figure S6, Table S5). For example, the top-ranked gene *IL17C* in PRP-dominated endotype E5 (Figure 4) is mainly expressed in keratinocytes, and elevated IL-17C protein levels has been associated with PRP disease severity[35]. In contrast, *TLR7* which is strongly upregulated in the interface-dominated endotype E4, has emerged as a therapeutic target in systemic lupus erythematosus, highlighting interferon-driven inflammation as a defining feature of this endotype[36].

Lower accuracy in E8 reflected its dispersed UMAP distribution (Figure 2E), higher intra-cluster variance, and greater similarity to other clusters (Table S6), suggesting a heterogeneous or transitional state. Demonstrating the clinical value of our endotype-based classifiers requires validation in independent patient cohorts, and we therefore assessed their performance using three gene expression datasets from psoriasis patients (two publicly available, one unpublished, Figure 5D, Table S7)[37, 38], of which each data set included skin biopsies taken at baseline.

Across all datasets, cases consistently mapped to E11–E13 and E5, confirming robustness (Figure 5D). Using available clinical data in these data sets (PASI, PGA), we assessed therapy responses across endotypes (Figure 5E, Figure S10). E12 showed the strongest response to IL-23 inhibition (OR 2.64), confirming the primary cohort. TNF inhibitors were most effective in E5, and IL-17 inhibition showed strongest effects in E13. Despite limited sample sizes, consistent trends across cohorts support the clinical relevance of endotype-based stratification. Overall, these results highlight the potential of molecular endotyping to predict treatment response and guide therapeutic decision-making in inflammatory skin diseases.

Discussion

Despite advances in targeted therapies, precision medicine in inflammatory skin diseases remains limited, with treatment decisions still largely based on trial and error. Here, we present a hypothesis-free molecular framework that classifies ncISDs into biologically defined endotypes, integrating transcriptomics and deep phenotyping to capture heterogeneity beyond diagnosis or immune patterns and enable therapeutic stratification.

A key finding is a previously unrecognized axis separating immune-dominated endotypes from those driven by metabolic and epidermal structural processes. While immune stratification underlies current therapies, grouping diseases by lipid metabolism, keratinocyte differentiation, and barrier integrity represents a conceptual shift, highlighting non-immune, tissue-intrinsic drivers.

This framework transcends both traditional diagnoses and immune-pattern classifications[10, 12]. Patients with different diseases often converge on shared endotypes, while those with the same diagnosis can diverge. For example, eczema spans nearly all endotypes, confirming its heterogeneity, while distinct diseases (e.g., eczema, granuloma annulare, pyoderma gangrenosum, cutaneous lymphoma) can share molecular programs, supporting cross-indication therapies[39, 40]. Importantly, this convergence was observed despite deep clinical phenotyping and inclusion of distinct clinicopathologic subentities rather than broad diagnostic labels alone. Even patients with highly similar clinicopathologic phenotypes exhibited distinct molecular endotypes and divergent therapeutic responses, suggesting that clinical morphology alone does not fully capture the underlying therapeutic biology. Therefore, this framework may enable molecular endotype-based basket-trial designs across conventionally distinct ncISDs sharing convergent pathogenic mechanisms. Our approach provides higher granularity, with 13 endotypes explaining more transcriptomic variance than diagnosis or immune patterns. Even within psoriasis, distinct endotypes reflect different drivers, from IL-23–mediated inflammation to keratinization processes. Residual heterogeneity (e.g., E8) suggests additional influences such as genetics, microbiome, and environment. Future integration of these dimensions may further refine endotypes and enhance predictive accuracy. In addition, several less common ncISDs were represented by comparatively small patient numbers. These entities were included to broaden the spectrum of inflammatory programs represented across the cohort rather than to establish disease-specific molecular subclassifications for rare diseases. Larger future cohorts will be required to further refine endotypes in less frequent ncISDs. To address these challenges, the Freiburg Translational Dermatology Initiative is prospectively collecting longitudinal deep-phenotyping and multi-omics data across the spectrum of chronic inflammatory skin diseases, providing a framework to validate, refine, and extend molecular endotypes toward prediction of clinically meaningful outcomes such as therapeutic response, disease progression, and comorbidity development[41].

Recently, Gilliet and colleagues proposed a module-based taxonomy that groups inflammatory skin diseases by shared immune-response patterns, marking an important shift toward mechanism-oriented classification beyond clinical phenotypes[13]. Our work complements and extends this framework by providing a hypothesis-free, data-driven classification rather than a classification anchored to immune modules curated by disease groups. Moreover, we integrate comprehensive clinical and histological metadata directly into molecular analyses, enabling direct linkage between biological programs and clinical attributes. Third, we reveal that immune activation alone does not fully explain ncISD heterogeneity and identify metabolic and structural epidermal programs as equally important disease-defining axes. Together, these advances move the field closer to a unified, mechanistic disease ontology that encompasses both immune and tissue-intrinsic drivers.

Clinically, psoriasis illustrates the relevance: despite effective TNF-, IL-17-, and IL-23–targeted therapies[32], predictive biomarkers are lacking[33, 34]. We show that psoriasis segregates into endotypes with distinct therapy responses, validated across independent cohorts. E12 responded best to IL-23 inhibition, while E5 and E13 favored TNF and IL-17 blockade. Importantly, the proposed endotypes can be predicted using a compact 25-gene classifier, enabling clinical implementation via automated PCR systems in the future[42]. Such classifiers may ultimately be implemented as low-dimensional and cost-effective point-of-care assays. Their clinical utility will need to be evaluated prospectively against standard clinical treatment selection, particularly given the substantial costs associated with ineffective biologic therapy.

While this study focused on ncISDs, the conceptual framework is broadly applicable to other inflammatory diseases characterized by clinical heterogeneity and incomplete therapeutic response, including asthma, inflammatory bowel diseases and rheumatologic conditions.

In summary, we define a molecular endotype-based classification that transcends diagnosis, explains heterogeneity, and informs therapy. By integrating immune and tissue-intrinsic

drivers and providing practical classifiers, this work establishes a foundation for precision medicine in dermatology and beyond.

Data and materials availability:

Bulk RNA-seq data generated in this study (study cohort "Germany South") have been deposited in NCBI GEO Database under accession number GSE308055. Accession numbers for the Validation cohort "Germany North" are GSE301106, for the Validation cohort for "USA East Coast" GSE106992 and for the Validation cohort for "USA North": NCT01971346 (clinicaltrials.gov).

The code can be found here: https://github.com/MendenLab/ncisd_endotypes

References

1. Davies H, Bignell GR, Cox C, Stephens P, Edkins S, Clegg S, et al. Mutations of the BRAF gene in human cancer. Nature 2002; 417:949-54.
2. Dean L, Kane M. Dabrafenib Therapy and BRAF Genotype. 2017.
3. Hebra F. On diseases of the skin, including the exanthemata: New Sydenham Society; 1868.
4. Shrank WH, Rogstad TL, Parekh N. Waste in the US Health Care System: Estimated Costs and Potential for Savings. JAMA 2019; 322:1501-9.
5. Karimkhani C, Dellavalle RP, Coffeng LE, Flohr C, Hay RJ, Langan SM, et al. Global Skin Disease Morbidity and Mortality: An Update From the Global Burden of Disease Study 2013. JAMA Dermatol 2017; 153:406-12.
6. Schabitz A, Eyerich K, Garzorz-Stark N. So close, and yet so far away: The dichotomy of the specific immune response and inflammation in psoriasis and atopic dermatitis. J Intern Med 2021; 290:27-39.
7. Lauffer F, Eyerich K. Eczematized psoriasis - a frequent but often neglected variant of plaque psoriasis. J Dtsch Dermatol Ges 2023; 21:445-53.
8. Bohner A, Jargosch M, Muller NS, Garzorz-Stark N, Pilz C, Lauffer F, et al. The neglected twin: Nummular eczema is a variant of atopic dermatitis with codominant T(H)2/T(H)17 immune response. J Allergy Clin Immunol 2023; 152:408-19.
9. Seremet T, Di Domizio J, Girardin A, Yatim A, Jenelten R, Messina F, et al. Immune modules to guide diagnosis and personalized treatment of inflammatory skin diseases. Nature communications 2024; 15:10688.
10. Eyerich K, Eyerich S. Immune response patterns in non-communicable inflammatory skin diseases. J Eur Acad Dermatol Venereol 2018; 32:692-703.
11. Schett G, McInnes IB, Neurath MF. Reframing Immune-Mediated Inflammatory Diseases. Reply. N Engl J Med 2021; 385:e75.
12. Garzorz-Stark N, Weidinger S, Sticherling M, Ghoreschi K, Enk A, Eyerich K. Inflammatory Skin Diseases: The Importance of Immunological Signatures. Dtsch Arztebl Int 2025; 122:277-82.
13. Seremet T, Di Domizio J, Girardin A, Yatim A, Jenelten R, Messina F, et al. Immune modules to guide diagnosis and personalized treatment of inflammatory skin diseases. Nat Commun 2024; 15:10688.
14. Seiringer P, Garzorz-Stark N, Eyerich K. T-Cell–Mediated Autoimmunity: Mechanisms and Future Directions. J Invest Dermatol 2022; 142:804-10.
15. Satija R, Farrell JA, Gennert D, Schier AF, Regev A. Spatial reconstruction of single-cell gene expression data. Nat Biotechnol 2015; 33:495-502.
16. Zheng GX, Terry JM, Belgrader P, Ryvkin P, Bent ZW, Wilson R, et al. Massively parallel digital transcriptional profiling of single cells. Nat Commun 2017; 8:14049.
17. Traag VA, Waltman L, van Eck NJ. From Louvain to Leiden: guaranteeing well-connected communities. Sci Rep 2019; 9:5233.
18. Pedregosa F, Varoquaux G, Gramfort A, Michel V, Thirion B, Grisel O, et al. Scikit-learn: Machine learning in Python. the Journal of machine Learning research 2011; 12:2825-30.
19. Roy P, Mandal J. Performance evaluation of some clustering indices. Computational Intelligence in Data Mining-Volume 3: Proceedings of the International Conference on CIDM, 20-21 December 2014: Springer, 2014:509-17.
20. Hegyi Z, Zwicker S, Bureik D, Peric M, Koglin S, Batycka-Baran A, et al. Vitamin D analog calcipotriol suppresses the Th17 cytokine-induced proinflammatory S100 "alarmins" psoriasin (S100A7) and koebnerisin (S100A15) in psoriasis. J Invest Dermatol 2012; 132:1416-24.
21. Zhang Y, Wang L, Sun X, Li F. SERPINB4 Promotes Keratinocyte Inflammation via p38MAPK Signaling Pathway. J Immunol Res 2023; 2023:3397940.

22. Marshall A, Celentano A, Cirillo N, McCullough M, Porter S. Tissue-specific regulation of CXCL9/10/11 chemokines in keratinocytes: Implications for oral inflammatory disease. PLoS One 2017; 12:e0172821.
23. Dhanani KCH, Samson WJ, Edkins AL. Fibronectin is a stress responsive gene regulated by HSF1 in response to geldanamycin. Sci Rep 2017; 7:17617.
24. Lauffer F, Jargosch M, Krause L, Garzorz-Stark N, Franz R, Roenneberg S, et al. Type I Immune Response Induces Keratinocyte Necroptosis and Is Associated with Interface Dermatitis. J Invest Dermatol 2018; 138:1785-94.
25. Shao S, Tsoi LC, Sarkar MK, Xing X, Xue K, Uppala R, et al. IFN-gamma enhances cell-mediated cytotoxicity against keratinocytes via JAK2/STAT1 in lichen planus. Sci Transl Med 2019; 11.
26. Maintz L, Welchowski T, Herrmann N, Brauer J, Traidl-Hoffmann C, Havenith R, et al. IL-13, periostin and dipeptidyl-peptidase-4 reveal endotype-phenotype associations in atopic dermatitis. Allergy 2023.
27. Kim J, Ahn K. Atopic dermatitis endotypes: knowledge for personalized medicine. Curr Opin Allergy Clin Immunol 2022; 22:153-9.
28. Akiyama M, Takeichi T, McGrath JA, Sugiura K. Autoinflammatory keratinization diseases. J Allergy Clin Immunol 2017; 140:1545-7.
29. Amar Y, Rogner D, Silva RL, Foesel BU, Ud-Dean M, Lagkouvardos I, et al. Darier's disease exhibits a unique cutaneous microbial dysbiosis associated with inflammation and body malodour. Microbiome 2023; 11:162.
30. Akech J, Wixted JJ, Bedard K, van der Deen M, Hussain S, Guise TA, et al. Runx2 association with progression of prostate cancer in patients: mechanisms mediating bone osteolysis and osteoblastic metastatic lesions. Oncogene 2010; 29:811-21.
31. Liu C, He S, Zhang J, Li S, Chen J, Han C. Silencing TCF4 Sensitizes Melanoma Cells to Vemurafenib Through Inhibiting GLUT3-Mediated Glycolysis. Onco Targets Ther 2020; 13:4905-15.
32. Sbidian E, Chaimani A, Guelimi R, Garcia-Doval I, Hua C, Hughes C, et al. Systemic pharmacological treatments for chronic plaque psoriasis: a network meta-analysis. Cochrane Database Syst Rev 2023; 7:CD011535.
33. Konrad RJ, Higgs RE, Rodgers GH, Ming W, Qian YW, Bivi N, et al. Assessment and Clinical Relevance of Serum IL-19 Levels in Psoriasis and Atopic Dermatitis Using a Sensitive and Specific Novel Immunoassay. Sci Rep 2019; 9:5211.
34. Corbett M, Ramessur R, Marshall D, Acencio ML, Ostaszewski M, Barbosa IA, et al. Biomarkers of systemic treatment response in people with psoriasis: a scoping review. Br J Dermatol 2022; 187:494-506.
35. Strunck JL, Cutler B, Rajpal B, Kent G, Haynes D, Topham CA, et al. Pityriasis Rubra Pilaris Response to IL-17A Inhibition Is Associated with IL-17C and CCL20 Protein Levels. J Invest Dermatol 2022; 142:235-9 e1.
36. Alper P, Betschart C, Andre C, Boulay T, Cheng D, Deane J, et al. Discovery of the TLR7/8 Antagonist MHV370 for Treatment of Systemic Autoimmune Diseases. ACS Med Chem Lett 2023; 14:1054-62.
37. Tsoi LC, Patrick MT, Shuai S, Sarkar MK, Chi S, Ruffino B, et al. Cytokine responses in nonlesional psoriatic skin as clinical predictor to anti-TNF agents. J Allergy Clin Immunol 2022; 149:640-9 e5.
38. Brodmerkel C, Li K, Garcet S, Hayden K, Chiricozzi A, Novitskaya I, et al. Modulation of inflammatory gene transcripts in psoriasis vulgaris: Differences between ustekinumab and etanercept. J Allergy Clin Immunol 2019; 143:1965-9.
39. Song EJ, Bezecny J, Farrer S. Recalcitrant generalized granuloma annulare treated successfully with dupilumab. JAAD Case Reports 2021; 7:1-2.
40. Pousti BT, Jin A, Sklovar L, Savage KT, Zhai LL, Mollanazar NK, et al. Dupilumab for the treatment of lichen planus. Cutis 2021; 107:E8-E10.

41. Jonsson P, Pilz AC, Maboudi H, Ranzinger D, Wagner P, Schaffert-Stone L-N, et al. The Translational dermatology initiative: Aiming at a new disease classification of inflammatory skin diseases. JID Innovations 2025; 5:100381.
42. Schmitt A, Proksch S, Gutzweiler L, Roth S, Engler M, Muller CSL, et al. Diagnostic concordance of dermatopathology and PCR in differentiating eczema from psoriasis. J Eur Acad Dermatol Venereol 2026.

608 **Tables**

Pattern	Disease	Samples (n)	Patients (n)	Age (mean age in years ± SD)	Sex (% of male)
1	Lichen planus	29	29	57.4 ± 14.3	41.4
	Lupus erythematosus	11	11		
	Lupus erythematosus unspecified	1	1	70.0 ± NA	0
	Chilblain lupus erythematosus	1	1	17.0 ± NA	100
	Chronic discoid lupus erythematosus	5	5	48.6 ± 19.6	20
	Subacute cutaneous lupus erythematosus	4	4	54.5 ± 9.9	25
	Lichenoid drug reaction	1	1	70.0 ± NA	0
2a	Eczema	123	121	54.1 ± 19.2	
	Eczema unspecified	11	11	57.6 ± 24.4	63.6
	Asteatotic eczema	3	3	70.3 ± 17.7	66.7
	Atopic dermatitis	39	39	43.8 ± 17.7	64.1
	Erythrodermic eczema	1	1	65.0 ± NA	100
	Hyperkeratotic rhagadiform hand eczema	4	3	50.2 ± 15.4	100
	Nummular eczema	62	62	58.3 ± 17.5	64.5
	Rosacea-like dermatitis	1	1	54.0 ± NA	100
	Seborrheic eczema	1	2	51.0 ± 0.0	100
	Prurigo simplex subacuta	1	1	89.0 ± NA	0
2b	Bullous pemphigoid	2	2	79.5 ± 12.6	50
3	Psoriasis	128	126		
	Plaque psoriasis	111	110	51.6 ± 16.2	67.6
	Guttate psoriasis	9	9	43.3 ± 18.0	55.6
	Inverse psoriasis	5	4	65.6 ± 16.8	20
	Palmoplantar psoriasis	3	3	50.3 ± 15.0	0
	Pityriasis rubra pilaris	14	14	61.6 ± 9.0	71.4
4a	Morphea	2	2	78.0 ± 5.7	0
	Venous ulcer	2	2	51.5 ± 40.3	100
	Systemic sclerosis	1	1	62.0 ± NA	0
4b	Granuloma annulare	2	2	57.5 ± 14.8	50
	Sarcoidosis	1	1	40.0 ± NA	100
5	Pustular psoriasis	9	9		
	Generalized pustular psoriasis	2	2	41.5 ± 20.5	0
	Palmoplantar pustular psoriasis	7	7	40.4 ± 14.2	57.1
	Pyoderma gangrenosum	12	11	55.5 ± 20.0	36.4
UD	Cutaneous lymphoma	19	19		
	Stage IA	18	18	71.6 ± 14.2	61.1
	Stage IVA1	1	1	85.0 ± NA	100
	Cutaneous side effects of biologics	11	11		
	Unspecified	2	2	46.0 ± 12.7	0
	Eczema unspecified	2	2	38.0 ± 7.1	50
	Hyperkeratotic rhagadiform hand eczema	1	1	62.0 ± NA	100

Cutaneous lupus erythematosus unspecified	1	1	39.0 ± NA	100
Nummular eczema	1	1	44.0 ± NA	100
Palmoplantar psoriasis	1	1	42.0 ± NA	0
Generalized pustular psoriasis	2	2	35.5 ± 14.8	0
Palmoplantar pustular psoriasis	1	1	23.0 ± NA	100
Darier's disease	10	10	43.5 ± 17.3	50
Keratosis lichenoides chronica	1	1	61.0 ± NA	100
Erythrodermia	2	2	59.9 ± 21.9	50
Pityriasis rosea	1	1	44.0 ± NA	100
Parapsoriasis	12	12	60.0 ± 12.4	75
non-lesional skin	333	332	54.2 ± 17.9	58.9

609

610 **Table 1: Composition of the study cohort, including 22 ncISDs assigned to their**

611 **respective immune response patterns.** Clinical subdiagnoses are shown where applicable.

612 The table provides the number of samples and patients, together with demographic

613 characteristics (age and sex) for each disease entity and subdiagnosis.

614

615

Figure Legends

Figure 1: Shortcomings of the traditional disease ontology and of immune-response patterns in predicting treatment outcomes. **A)** Overview of the study cohort comprising 390 patients suffering from 22 non-communicable inflammatory skin diseases (ncISDs). Exemplary gene expression profiles of eczema patients are shown for lesional (LS) and non-lesional (NL) skin, based on transcriptomic data generated from all patients' lesional and non-lesional skin. **B)** Heatmap of 86 imputed and scaled attributes characterizing patients' clinical phenotypes. Exemplarily shown for all attributes (boxed at higher magnification) are attributes from routine histology such as "Neutrophils" as well as from assessed comorbidities such as "Arthritis". **C)** 2D UMAP representation of patients' skin transcriptomes according to diagnosis (color code as in A). Each dot represents one patient. **D)** UMAP representation of patients' skin transcriptomes according to immune response patterns. Each dot represents one patient. **E)** 2D UMAP representation of patients according to phenomics reveals intermingled clusters of ncISDs. Each dot represents one patient (color code as in A). **F)** Radar plots show representative examples of the phenomic profiles of two plaque-type psoriasis patients and one pustular psoriasis patient before and after anti-IL-17 treatment.

Figure 2: Identification of disease endotypes. A-D) Workflow of the identification of endotypes. A) Immune-response patterns 1, 2a, 3 and 5 were used to guide endotype identification. B) Genes were ranked using the Cluster-Informative Featured Genes method described in Supplementary Methods. C) The optimal proportion of genes was determined by applying cross-validation and performing Leiden clustering across datasets containing varying percentages of genes. For each clustering, the distribution of predominant immune-response patterns was evaluated, and the corresponding pattern score was computed. D) An optimal

641 subset comprising 7% of the genes was identified for endotype definition, yielding a mean
642 pattern score of 72.22. E) 2D representation of identified disease endotypes. F) Grouping of
643 ncISDS into patterns and endotypes. G) Variance partition analysis comparing the proportion
644 of transcriptomic variance explained by endotypes, diagnoses, and patterns. E: endotype; UD:
645 undefined

646

647 **Figure 3: Hierarchical organization of ncISD endotypes. A)** Hierarchical clustering tree of
648 the 13 non-communicable inflammatory skin disease (ncISD) endotypes based on molecular
649 profiles. Each node indicates a split in endotype structure, annotated with the most
650 representative signaling pathways and biological processes identified at each branching level.
651 Bar plots show the distribution of clinical diagnoses (top row) and patterns (bottom row)
652 across endotypes. **B-D)** The branches at the highest level (diamond) divide the structural and
653 metabolism arm (yellow) from the inflammation arm (red) with top differentiating genes for
654 E5–E10 versus E1-4 and E11–E13 (B). The inflammation arm (circle) can be further divided
655 into a psoriasis-like endotype branch (violet) and a branch comprising autoinflammatory and
656 interface dermatitis diseases (blue) with top differentiating genes for E1-4 versus E11–E13
657 (C). The latter branch (triangle) is split again into autoinflammatory (sandy brown) and
658 interface dermatitis disease (light green) branches with top differentiating genes for E11-E2
659 versus E3-E4 (D).

660

661 **Figure 4: Molecular network of endotype interaction. A)** Interaction network of endotype
662 E5, E11, E12 and E13 including endotype-specific top pathways, regulated key genes per
663 endotype, transcription factor target sets and associated phenotypic attributes. Dot size
664 represents the categorized effect size of phenotypic attributes (small, medium, or large):
665 Cohen's d for continuous variables, Cliff's delta for ordinal categories, and odds ratio for

nominal categories. The color indicates the signed $-\log_{10}$(p-adjusted) value from statistical testing, with blue tones indicating negative associations and red tones indicating positive associations. **B)** Responders and non-responders to the commonly administered biologics anti-IL-17, anti-TNF and anti-IL23. Boxplots depict the delta PGA and PASI score for patients with the psoriasis endotypes E5, E11-E13 for each drug targeting TNF, IL-23, and IL-17. The dashed line visualizes treatment success, corresponding to a delta PGA/PASI score ≥ 0.5.

Figure 5: **Performance of molecular classifier and validation of molecular classifier in independent cohorts**. **A)** Classification accuracy of support vector classifiers (SVC) as a function of the number of selected genes per endotype. The red dot marks the peak performance with accuracy of 81.4% ± 7.5% using131 genes per endotype. **B)** Confusion matrix averaged over 20-fold cross-validation. Rows represent true endotype labels, columns represent predicted labels. Mean overall accuracy, standard deviation and number of genes used are indicated. **C)** Heatmap showing expression patterns of the top-ranked genes used for endotype classification. Genes were selected by differential expression analysis (Discriminative Featured Genes, DFG) and are hierarchically clustered. Expression values are normalized per gene. **D)** Distribution of patients' gene expression profiles across endotypes for which phenomic data on therapy response data on anti-IL-17, anti-TNF and anti-IL23 therapy was available. Dot size corresponds to the number of patients in each endotype, while geographical maps symbolize origin of data sets ((USA East Coast, Germany North, Germany South (our cohort), USA North)). **E)** Forest plots show odds ratios (OR) with 95% confidence intervals comparing treatment response in each endotype individually (E5, E11, E12, E13) against the pooled remainder of the cohort (e.g., E5 vs E11/E12/E13) for IL-23–, TNF-, and IL-17–directed therapies. The vertical dashed line indicates no difference in response (OR = 1).

Patient-specific attributes		
Nominal	**Ordinal**	**Continuous**
Comorbidity arthritis (dichotome)	Morphology erythema (1-3)	Histology Hyerkeratosis (quantitative)
Comorbidity uveitis (dichotome)	Morphology elevation/infiltration (1-3)	Histology Parakeratosis (quantitative)
Comorbidity arterial hypertension (dichotome)	Morphology papules (1-3)	Histology Orthokeratosis (quantitative)
Comorbidity infection-associated exacerbation	Morphology vesicles (1-3)	Histology acanthosis (quantitative)
Comorbidity allergic rhinoconjunctivitis (dichotome)	Morphology pustules (1-3)	Histology spongiosis (quantitative)
Comorbidity diabetes mellitus (dichotome)	Morphology scaling (1-3)	Histology dilated capillaries (quantitative)
Comorbidity bronchial asthma (dichotome)	Morphology dryness (1-3)	Histology lymphocytes dermal (quantitative)
Comorbidity hepatitis (dichotome)	Histology Suprapapillar Epidermis (qualitative)	Histology exocytosis of lymphocytes (quantitative)
Comorbidity renal insufficiency (dichotome)	Histology Parakeratosis (qualitative)	Histology neutrophils (quantitative)
Comorbidity recurrent tonsillitis (dichotome)	Histology Acanthosis (qualitative)	Histology eosinophils (quantitative)
Comorbidity inflammatory bowel disease (dichotome)	Histology granulosis (qualitative)	Histology interface dermatitis (quantitative)
Comorbidity nails involved (dichotome)	Histology serum crust (qualitative)	Histology leukocytoclastic vasculitis (quantitative)
Comorbidity mucosa involved (dichotome)	Histology maximal distribution of lymphocytes dermal (qualitative)	Histology mucin (quantitative)
Comorbidity scalp involved (dichotome)	Histology microabscess (qualitative)	Laboratory leukocytes (number)
History family history (dichotome)	Histology bacteria (qualitative)	Laboratory hemoglobin (number)
History exanthematic (dichotome)	Histology neutrophils (qualitative)	Laboratory lymphocytes (number)
History self limited (dichotome)	Histology suprabasal dyskeratoses (qualitative)	Laboratory neutrophil granulocytes (number)
History photosensitivity (dichotome)	Histology distribution of dyskeratoses (qualitative)	Laboratory eosinophils (number)
History progessive (dichotome)	Histology interface dermatitis (qualitative)	Laboratory serum creatinine (number)
History smoking (dichotome)	Histology number of dyskeratoses at hotspot (40x)	Laboratory GPT (number)
Laboratory culture staphylococcus aures (dichotome)	History sport (1-3)	Laboratory total IgE (number)
Laboratory specific IgE (dichotome)	History alcohol consumption (1-3)	Comorbidity body mass index (number)
Sex	History onset in life	History weeks since onset (number)
Therapeutic target	History pruritus	Age
	PGA (physician's global assessment, 0-4)	Therapy PGA x weeks after start of the therapy
	PASI (psoriasis area and severity index, 0-72)	Therapy leukocytes
	SCORAD (scoring atopic dermatitis, 0-103)	Therapy hemoglobin
	DLQI (dermatology life quality index, 0-30)	Therapy lymphocytes
	Therapy degree of response (1-4)	Therapy neutrophil granulocytes
	Therapy speed of response (1-3)	Therapy eosinophils
		Therapy serum creatinine
		Therapy GPT

Disease	Drug								
	IL-4RA (dupilumab)	**IL-13 (tralokinumab, lebrikizumab)**	**CD20 (rituximab)**	**IgE (omalizumab)**	**TNF-a (adalimumab, infliximab)**	**IL-17 (secukinumab, ixekizumab)**	**IL-23 (guselkumab, risankizumab)**	**IL-1 (anakinra, canakinumab)**	**IL-6 (Tocilizumab)**
Lichen planus	1 case report with improvement [1], but also induction of lichen by dupilumab[2]	No reports, no clinical trials	0/5 patients improved [3]	No case reports, no clinical trials; induction of lichen by omalizumab reported[4]	No clinical trials, individual case reports of success [5], but also multiple cases of induction of disease[6]	RCT: secukinumab ineffective[7] case reports of success [8], however, can also induce disease [9]	1 case report with improvement [8], however, can also induce disease[10]	No case reports, no clinical trials	No case reports, no clinical trials
Lupus	No clinical trials; case reports of induction of disease [11]	No case reports, no clinical trials	Ineffective or weak efficacy on skin lesions [12]	Clinical trial completed, no results published (NCT01716312)	No clinical trials; multiple case reports of induction of disease [13]	Single cases with negative effects [14]; clinical trial withdrawn (NCT03866317)	No clinical trials; ustekinumab trial terminated (NCT03517722)	No case reports, no clinical trials	Abandoned after phase 2 trial (NCT01273389)
Pityriasis rubra pilaris	No case reports, no clinical trials	No case reports, no clinical trials	No case reports, no clinical trials	No case reports, no clinical trials	Only case series: 50% of patients improve ≥75% [15]	40% -55% of patients patients improve ≥75% [16] [17]	Active clinical trial, no results yet (NCT03975153), case reports of success [18]	No case reports, no clinical trials	No case reports, no clinical trials
Psoriasis	No clinical trials; multiple case reports of induction of disease [19]	No case reports, no clinical trials	No clinical trials; multiple case reports of induction of disease [20]	No case reports, no clinical trials	**40-80% of patients improve ≥75% [21]**	**65-72% of patients improve ≥90% [21]**	**65-72% of patients improve ≥90% [21]**	No clinical trials; one case report of induction of disease [22]	No clinical trials; multiple case reports of induction of disease [23]
Atopic dermatitis	**60% of patients improve ≥75% [24]**	**30 – 55% of patients improve ≥75% [24]**	Conflicting case series: 6/6 patients improved [25]; 0/2 patients improved [26]; 0/3 patients improved [27]	Conflicting case series with varying response from 0 to 100% of patients improving [28], no clinical trials	No clinical trials, case series: 2/9 patients improved ≥75% [29]	Ineffective (phase 2 trial) [30]; induction of disease in up to 12% of patients treated [31]	No reports of efficient treatment, no clinical trials running; ustekinumab inefficient [32]	Inefficient (clinical trials stopped without publication: NCT01122914)	3/3 patients improved ≥75% [33], no clinical trials
Nummular eczema	Mean improvement in case series with 30 patients: 90%,[34]; positive case report[35] clinical trial ongoing (NCT04600362)	No case reports, no clinical trials	No case reports, no clinical trials	No case reports, no clinical trials	No clinical trials; one case report of induction of disease [36]	No case reports, no clinical trials	No case reports, no clinical trials	No case reports, no clinical trials	No case reports, no clinical trials
Bullous pemphigoid	Clinical trial running (NCT04206553), multiple case reports and case series reporting success [37]	No case reports, no clinical trials	Multiple case reporst and case series reporting very good efficacy [38]	Multiple case reports and case series reporting very good efficacy [38]	No clinical trials; multiple case reports of induction of disease [39]	No clinical trials; case reports of induction of disease [40]	No clinical trials; case reports of induction of disease [40]	No case reports, no clinical trials	No case reports, no clinical trials
Granuloma annulare	One case report reporting success [41], no clinical trials	No case reports, no clinical trials	No case reports, no clinical trials	No case reports, no clinical trials	Multiple case reports and case series report efficacy in 80% of patients [42]; however, can also induce disease [9]	No clinical trials; 3 case reports of induction of disease [43]	No case reports, no clinical trials	No case reports, no clinical trials	No clinical trials; multiple case reports of induction of disease [44]
Sarcoidosis	No case reports, no clinical trials	No case reports, no clinical trials	No case reports, no clinical trials	No case reports, no clinical trials	50% of patients improve ≥50% [45]; however, can also induce disease [9]	No clinical trials; 5 case reports of induction of disease [9]	No case reports, no clinical trials	No clinical trials; 3 case reports of induction of disease [9]	No case reports, no clinical trials
Pustular Psoriasis	No clinical trials; case reports of induction of disease [46]	No clinical trials; case reports of induction of disease [46]	No clinical trials; case reports of induction of disease [47]	No case reports, no clinical trials	33% of patients (95% CI 12%-62%) achieve GPPGA score of 0 or 1 at week 8 [48]	54% of patients (95% CI 34%-74%) achieve GPPGA score of 0 or 1 at week 8 [48]	62% of patients (95% CI 35%-85%) achieve GPPGA score of 0 or 1 at week 8 [48]	50% of patients improve ≥50% after 12 weeks [49]	No clinical trials; multiple case reports of induction of disease [50]
Pyoderma gangrenosum	No clinical trials; case reports of induction of disease [51]	No case reports, no clinical trials	No clinical trials; case reports of induction of disease [52]	No case reports, no clinical trials	67% of patients (95% CI 62%-72%) achieve complete remission [53]	Conflicting case series, can also induce disease [54]	68%-71% of patients improve, case series [55]	38%-55% of patients improve, case series [56]	Conflicting cases, can also induce disease [57,58]

	Disease	Lichen planus	Lupus erythema-tosus	Lichenoid drug reaction	Eczema	Prurigo simplex subacuta	Bullous pemphigoid	Psoriasis (*PV, GP, IP, PPP*)	Pityriasis rubra pilaris	Morphea	Venous ulcer	Systemic sclerosis	Granuloma annulare	Sarcoidosis	Pustular psoriasis (*GPP, PPPP*)	Pyoderma gangrenosum	Cutaneous lymphoma	Cutaneous side effects of biologics	Darier disease	Keratosis lichenoides chronica	Erythro-dermia	Para-psoriasis
Endotype	E5	0	0	0	15	0	0	25 (*60, 40, 0, 0*)	45	0	0	0	0	0	5 (*100,0*)	0	5	0	0	0	5	0
	E6	0	0	0	33.33	0	0	5.56 (*100,0,0,0*)	11.11	0	0	0	0	0	0	0	0	5.56	38.89	0	0	5.56
	E7	4.76	0	2.38	71.43	2.38	2.38	14.29 (*83.3, 0,0, 16.7*)	0	0	0	0	0	0	2.38 (*0,100*)	0	0	0	0	0	0	0
	E8	0	0	0	44	0	0	48 (*66.7. 16.7. 8.3. 8.3*)	0	0	0	0	0	0	0	0	8	0	0	0	0	0
	E9	0	0	0	35.71	0	0	3.57 (*100,0,0,0*)	3.57	0	0	0	0	0	0	0	28.57	7.14	0	0	0	21.43
	E10	4.35	0	0	43.48	0	4.35	8.7 (*100,0,0,0*)	0	4.35	0	4.35	4.35	0	0	0	4.35	0	8.7	0	0	13.04
	E11	0	0	0	9.52	0	0	80.95 (*100,0,0,0*)	0	0	0	0	0	0	0	0	9.52	0	0	0	0	0
	E12	0	0	0	12.5	0	0	72.92 (*85.7, 8.6, 5.7, 0*)	2.08	0	0	0	0	0	2.08 (*0,100*)	0	0	4.17	2.08	0	2.08	2.08
	E13	0	0	0	3.23	0	0	87.1 (*81.5, 7.4, 7.4, 3.7*)	0	0	0	0	0	0	9.68 (*0,100*)	0	0	0	0	0	0	0
	E1	3.45	0	0	68.97	0	0	10.34 (*100,0,0,0*)	0	0	0	0	0	0	3.45 (*0,100*)	3.45	6.9	3.45	0	0	0	0
	E2	0	0	0	6.25	0	0	0	0	0	12.5	0	6.25	6.25	0	62.5	6.25	0	0	0	0	0
	E3	66.67	3.33	0	16.67	0	0	3.33 (*100,0,0,0*)	0	0	0	0	0	0	0	0	6.67	3.33	0	0	0	0
	E4	0	81.82	0	0	0	0	0	0	9.09	0	0	0	0	0	0	0	0	0	9.09	0	0

	Pattern	1	2a	2b	3	4a	4b	5	UD
Endotype	E5	0	15	0	70	0	0	5	10
	E6	0	33.33	0	16.67	0	0	0	50
	E7	7.14	73.81	2.38	14.29	0	0	2.38	0
	E8	0	44	0	48	0	0	0	8
	E9	0	35.71	0	7.14	0	0	0	57.14
	E10	4.35	43.48	4.35	8.7	8.7	4.35	0	26.09
	E11	0	9.52	0	80.95	0	0	0	9.52
	E12	0	12.5	0	75	0	0	2.08	10.42
	E13	0	3.23	0	87.1	0	0	9.68	0
	E1	3.45	68.97	0	10.34	0	0	6.9	10.34
	E2	0	6.25	0	0	12.5	12.5	62.5	6.25
	E3	70	16.67	0	3.33	0	0	0	10
	E4	81.82	0	0	0	9.09	0	0	9.09

No	Pattern	Endotype	Diagnosis	Therapy	Therapeutic target	Score	W0	W12 after initiation	Delta PASI Rate W12	Delta PGA Rate W 12	Result W12
1	3	E11	Psoriasis	Secukinumab	IL-17	PASI	35.2	10.9	0.7		Non_responder
2	3	E11	Psoriasis	Ixekizumab	IL-17	PASI	10.6	1.6	0.8		Responder
3	3	E11	Psoriasis	Secukinumab	IL-17	PASI	12.5	0.0	1.0		Super_responder
4	3	E11	Psoriasis	Secukinumab	IL-17	PASI	2	0.0	1.0		Super_responder
5	3	E11	Psoriasis	Ixekizumab	IL-17	PASI	16.1	0.5	1.0		Super_responder
6	3	E11	Psoriasis	Guselkumab	IL-23	PASI	16.4	5.2	0.7		Non_responder
7	3	E11	Psoriasis	Guselkumab	IL-23	PASI	16.9	3.6	0.8		Responder
8	3	E11	Psoriasis	Guselkumab	IL-23	PASI	19.8	0.4	1.0		Super_responder
9	3	E11	Psoriasis	Infliximab	TNF	PASI	17.8	7.6	0.6		Non_responder
10	3	E11	Psoriasis	Infliximab	TNF	PASI	14.3	5.8	0.6		Non_responder
11	3	E11	Psoriasis	Infliximab	TNF	PASI	36.8	3.9	0.9		Responder
12	3	E11	Psoriasis	Remicade	TNF	PASI	21	1.7	0.9		Super_responder
13	3	E12	Psoriasis	Secukinumab	IL-17	PASI	12	1.5	0.9		Responder
14	3	E12	Psoriasis	Secukinumab	IL-17	PASI	8.4	7.0	0.2		Super_nonresponder
15	3	E12	Psoriasis	Ixekizumab	IL-17	PASI	1.2	1.0	0.2		Super_nonresponder
16	3	E12	Psoriasis	Secukinumab	IL-17	PGA	1	1.0		0	Super_nonresponder
17	3	E12	Psoriasis	Secukinumab	IL-17	PASI	24.2	2.0	0.9		Super_responder
18	3	E12	Psoriasis	Ustekinumab	IL-23	PASI	6.6	4.2	0.4		Non_responder
19	3	E12	Psoriasis	Guselkumab	IL-23	PASI	5.9	2.0	0.7		Non_responder
20	3	E12	Psoriasis	Risankizumab	IL-23	PASI	13.8	2.2	0.8		Responder
21	3	E12	Psoriasis	Guselkumab	IL-23	PASI	20.6	1.8	0.9		Super_responder
22	3	E12	Psoriasis	Guselkumab	IL-23	PASI	34.1	1.2	1.0		Super_responder
23	3	E12	Psoriasis	Risankizumab	IL-23	PASI	15	1.2	0.9		Super_responder
24	3	E12	Psoriasis	Risankizumab	IL-23	PASI	34.3	1.4	1.0		Super_responder
25	3	E12	Psoriasis	Adalimumab	TNF	PASI	15	10.0	0.3		Non_responder
26	3	E12	Psoriasis	Adalimumab	TNF	PASI	8.2	5.0	0.4		Non_responder
27	3	E12	Psoriasis	Adalimumab	TNF	PASI	13	7.1	0.5		Non_responder
28	3	E12	Psoriasis	Infliximab	TNF	PASI	42.1	10.0	0.8		Responder
29	3	E12	Psoriasis	Infliximab	TNF	PGA	4	4.0		0	Super_nonresponder
30	3	E13	Psoriasis	Secukinumab	IL-17	PASI	16.2	3.1	0.8		Responder
31	3	E13	Psoriasis	Secukinumab	IL-17	PASI	25	20.2	0.2		Super_nonresponder
32	3	E13	Psoriasis	Secukinumab	IL-17	PASI	28	1.8	0.9		Super_responder
33	3	E13	Psoriasis	Guselkumab	IL-23	PASI	11.1	2.2	0.8		Responder
34	3	E13	Psoriasis	Guselkumab	IL-23	PASI	27.9	1.8	0.9		Super_responder
35	3	E13	Psoriasis	Infliximab	TNF	PASI	20.9	4.5	0.8		Responder
36	3	E13	Psoriasis	Infliximab	TNF	PASI	22.4	4.2	0.8		Responder
37	3	E13	Psoriasis	Remicade	TNF	PASI	19.4	1.7	0.9		Super_responder
38	UD	E4	Keratosis lichenoides chronica	Infliximab	TNF	PGA	4	2.0		0.5	Non_responder
39	3	E5	Pityriasis rubra pilaris	Guselkumab	IL-23	PGA	5	3.0		0.4	Non_responder
40	3	E5	Pityriasis rubra pilaris	Guselkumab	IL-23	PGA	4	1.0		0.75	Responder
41	3	E6	Psoriasis	Guselkumab	IL-23	PASI	14.3	1.9	0.9		Responder
42	3	E7	Psoriasis	Secukinumab	IL-17	PGA	4	1.0		0.75	Responder
43	3	E7	Psoriasis	Guselkumab	IL-23	PASI	21.2	5.1	0.8		Responder
44	3	E7	Psoriasis	Adalimumab	TNF	PASI	8	3.5	0.6		Non_responder
45	3	E8	Psoriasis	Secukinumab	IL-17	PASI	1.2	0.1	0.9		Super_responder
46	3	E8	Psoriasis	Brodalumab	IL-17	PASI	13.8	0.4	1.0		Super_responder
47	3	E8	Psoriasis	Guselkumab	IL-23	PGA	4	3.0		0.25	Non_responder
48	3	E8	Psoriasis	Adalimumab	TNF	PGA	4	1.0		0.75	Responder
49	3	E9	Pityriasis rubra pilaris	Brodalumab	IL-17	PGA	2	0.0		1	Super_responder
50	3	E9	Pityriasis rubra pilaris	Infliximab	TNF	PGA	4	2.0		0.5	Non_responder

Gene Rank	Endotype E1	E2	E3	E4	E5	E6	E7	E8	E9	E10	E11	E12	E13
1	PCSK1	ADAM12	CXCL9	IFIT2	PGLYRP2	KRT4	PPP1R3C	ACOT7	CENPP	ID4	KRT35	SLC23A2	CNNM4
2	TNC	COL11A1	FOXP3	HERC5	IL17C	PDE6A	KRTAP9-6	AGPAT3	KRT6B	SSBP2	KRTAP4-7	TNIP3	STS
3	CD209	COL10A1	RUNX3	CXCL11	CCL20	CIDEA	CD9	NADK	ADCY2	MTURN	KRT85	ADGRF1	GBA2
4	UAP1	SLC24A2	ZC3H12D	CD38	SERPINA6	UGT2A1	KRT27	FAM71B	KRT17	KRT16	KRT74	FERMT1	TDP2
5	CEMIP	MMP13	IL2RB	PLAAT2	EPOP	PNPLA5	COL6A6	MCRIP1	ATP2B4	S100A9	TCHH	KLK13	DUSP14
6	CLEC4G	INHBA	TRAF1	SP110	SLC11A2	MOGAT1	TCHH	CNDP2	CERS6	S100A8	KRTAP9-4	IDH3A	PLBD1
7	ADAMTS1	FN1	UBD	USP18	MINPP1	PNLDC1	KRT71	BROX	ANKRD33B	KRT6A	KRT25	AFAP1L2	TMPRSS11A
8	APELA	SPP1	SFTPA1	IFI35	C15orf62	SLC26A3	KRTAP2-2	CHST2	HIF1A	KPNA2	KRT71	NES	FCHSD1
9	ABL2	CCN4	TSPAN33	PLA1A	REN	ACSS2	KRT25	OPA3	SIPA1L2	LONRF1	KRT32	CFH	RAB5A
10	PDE4D	BCAT1	RUFY4	HSH2D	RALGAPA2	TLCD4	KRT74	ZNRD2	OR2G6	ARPC2	KRT27	SPTSSA	SPRR2F
11	IL24	SLC16A3	LAT	TRIM5	ATP12A	FDPS	ANO1	ARFRP1	ATG2B	GALNT6	KRTAP9-2	SUCO	KLK9
12	MEDAG	LOXL2	SEPTIN1	SP100	SERPINA3	GAL	IGFL4	POLR3H	KRT75	PTPN21	KRT82	FAM3D	ESYT3
13	FGF7	WNT2	CD6	ZBP1	PGLYRP4	AWAT2	ANXA4	SIPA1	ABHD6	ERBB4	KRTAP3-1	SPRR2F	CSTA
14	COL4A3	KIF26B	TNFRSF9	CMPK2	ATP6V1C2	ERV3-1	CD109	ARHGEF1	CDON	MARCHF6	MAN2A1	KLK6	SPRR2B
15	STEAP1	TDO2	FCRL3	EIF2AK2	LRG1	TMEM97	MAF	SCYL1	HECA	GHR	KRTAP9-8	FZD5	GBA
16	IL6	PLOD2	ZNF831	IFIT3	KCNJ18	UBIAD1	KRT85	WIZ	FABP5	WNT2B	KRT86	CLDN17	C10orf99
17	IL1R1	BMP8A	CTLA4	MX2	WWC1	ELOVL3	MARCKS	FDX2	CNTNAP3	ARFGEF3	KRT81	ZC3H12A	DEFB4A
18	STEAP2	CSMD2	CXCL10	CCL8	GFOD2	TRIM55	CXCR2	DUSP16	SMG1	BTC	FOXE1	SLC6A14	RNASE7
19	HTRA3	FGF5	TIFAB	IFIH1	MAPKAPK3	FAR2	LURAP1L	NPLOC4	FOXN3	MAGI1	KRT83	LIPG	ADIPOR2
20	SLC39A14	CXCL5	CD3G	IFIT5	CMTM6	SEC14L4	HRH1	FAM120A	GJB6	PRLR	KRTAP1-1	DEFB4A	FAM25A
21	PARD3	MMP14	TIGIT	RSAD2	ZNF662	MSMO1	CALHM4	DHX40	BCL11B	GJB2	KRTAP4-1	SHROOM2	SPTLC2
22	SERPINE2	RXFP1	CD27	ZNFX1	TRIM10	SLC25A18	FABP9	FAAP100	KCNJ15	SYDE2	KRT28	RCOR1	GDPD3
23	TCP11L2	POPDC3	CD2	IFIT1	SRCIN1	AWAT1	IL31RA	RBM10	N4BP2L1	RGMB	KRTAP3-2	TCN1	SPNS2
24	RAPGEFL1	MFAP2	GPR174	RNF114	ATP2C2	SGK2	KRTAP1-5	DUS1L	ZC2HC1A	SPATA6	KRTAP9-3	STAT3	CNFN
25	CYP19A1	RARRES2	IKZF3	PPM1K	SLC15A1	DGAT2L6	KRT26	RHBDF2	EFHC2	DMD	FRK	BTBD11	PLA2G4D
26	THBS1	TRPA1	LY9	NMI	UNC93A	SEC14L6	CCDC113	ASCC2	CCDC146	NOCT	PGBD5	TMPRSS11D	S100A12
27	NABP1	RUNX2	AKNA	OTOF	LIPK	CYB5A	KRTAP16-1	MPND	KRT6C	SEPTIN10	KRTAP9-9	SFXN3	GDA
28	MASP1	C1QTNF6	CD8A	SAMD9L	TNIP1	PDZK1	KRT82	SIRT6	ALDH3A2	RRM2	KRTAP11-1	FLG2	ACP7
29	MINDY1	MMP11	NLRC3	ISG20	ARSF	ACAT2	CORO6	CEP72	GJB2	WDR72	PSORS1C2	RHCG	SMURF2
30	COL4A4	P4HA1	CACNB4	BST2	GLB1L3	HAO2	MAP3K5	NDUFS8	SYNE2	MKI67	KRTAP4-12	PLAT	SPRR2G
31	IL1RL1	SULF1	SPN	XRN1	EREG	AADACL3	KRTAP5-11	SDF4	DDB2	TYMP	KRTAP5-2	PI3	GM2A
32	CCDC71L	DCSTAMP	ZNF366	SMCHD1	NKPD1	SEC14L3	CA2	SCAF1	ZNF273	LRP8	KRTAP1-5	ALDH1A3	IL36A
33	FBXO42	FHAD1	PPP1R16B	TDRD7	GBA	APMAP	TNFSF15	FGD3	CYSLTR2	PPM1A	KRT33B	NFKBIZ	RAI14
34	NNMT	COL24A1	ICOS	DDX58	NEU2	CRAT	C1QTNF1	HELZ2	CLEC2A	TMEM245	SH2D4A	CRABP2	SPRR2E
35	THEM5	FAP	ITGAL	TLR7	FRY	ROS1	IL13	SHKBP1	PGAM1	SIK2	KYNU	TGFA	FAM162A
36	ACKR3	MPP7	EOMES	AIM2	QPCT	ARR3	KRTAP17-1	UBALD1	ARID2	FAM189A2	KRTAP4-4	CARHSP1	ARG1
37	IL13RA2	FNDC1	CD3E	TRANK1	IL20	MOGAT2	CCL13	ARHGEF19	FBXW7	NPY1R	GDA	HEATR3	WASL
38	CCL2	LAMB1	CD5	PHF11	ACAD9	INSIG1	KRT33A	SHROOM1	MBTD1	ARNTL2	KRTAP26-1	XDH	JMY
39	OSMR	COL5A2	DUSP4	TRIM21	SLC5A1	RDH11	PLEKHA2	PNPLA6	CYP4F12	ZNF704	S100A3	ATL1	USP2
40	CFAP69	SERPINE1	ZAP70	IDO1	SLC35E1	BCAT2	KRT38	ZC2HC1A	WDR47	S100A7	KRTAP4-8	EPHA2	FBXO45
41	NR4A3	SLC2A5	CCL5	ADAR	TIAM1	ACADM	KRT35	AUP1	LRRC59	EPB41L4B	DSG4	CASP5	OTUB2
42	IGF1	ERBB3	MICAL1	LY6E	ELF3	ACSL1	DSG4	GCN1	TMPRSS11D	NTRK3	TGM6	MAML2	LCE3E
43	SLC39A8	TENM3	ACAP1	PLAC8	ACOX1	PMFBP1	TYR	COASY	SLC25A26	GARS1	LYG2	NOS2	TGM3
44	PDZD2	PLOD1	IL16	PARP12	PLA2G4B	PKLR	PMEL	NDUFA11	P2RY14	PGAM1	AASS	GM2A	IL36G
45	PI15	KCNJ6	HLA-DQB2	LAP3	ACP3	FA2H	ABLIM2	ATAD3B	SLC16A9	KLHDC2	KRTAP5-1	HDGF	PTGER3
46	CTSL	BGN	NLRC5	TRIM38	DMBT1	BRI3BP	CCL18	CCNE2	TARS1	ZNF577	MUC4	CAB39L	LCE3D

47	NTRK1	SLC11A1	SIT1	ISG15	PNPLA1	OLAH	LYG2	FOXK2	ARID1B	INHBB	KRTAP4-3	HRH2	YOD1
48	SPON1	CDH11	TMC8	BCL2L14	CDYL2	FADS2	CASP5	VAC14	VPS13D	PHYHD1	HRH2	SOST	DBI
49	CEMIP2	ARHGEF37	LCK	DHX58	SMPD1	UGT2A2	MLANA	CTNS	AFF1	EFHC1	ZC3H12A	RND1	LCE3A
50	MCCC1	IBSP	IL32	DTX3L	IL23A	PECR	SLC24A5	ARHGAP27	EPGN	ACADL	KRTAP24-1	CYB5R2	PLCD1
51	ACSL4	NEK6	APOBEC3G	STAT2	HMGA1	TMEM91	PAMR1	DESI1	SLC6A2	PLLP	B4GALNT2	CD24	WFDC12
52	BCL11A	CCDC102B	CD247	MEP1B	SHOC1	FBP2	NRIP1	AURKAIP1	DNAH11	TMEM50B	NOS2	KLK10	KLHL18
53	CES4A	RGS4	ADGRF1	TLR3	KIF13B	HGD	KRT28	DAPK3	PGD	EIF4A1	KRTAP2-1	PLS1	NT5C3A
54	RNF128	GRHL2	IRF8	CMTR1	MYO5B	PGRMC1	COL6A5	SLC38A10	OR2T10	SPRR1B	TCHHL1	ANKH	RAB25
55	NMNAT3	COL12A1	SKAP1	RTP4	ZNF532	TMPRSS11E	PTGDR2	TRIM28	SRXN1	CLDN8	HYAL4	IL36A	TMPRSS13
56	TPM4	FNDC3B	UCP2	DDX60L	SCNN1G	ACSBG1	KTN1	PDXK	LONRF1	SERPINB4	OLFM1	LCN2	SPRR2A
57	SCG2	LIMS1	HLA-DOB	IFITM1	SMPD3	AXDND1	IL17RB	UXS1	AGO4	ZNF606	KRT34	TMEM171	EIF6
58	NEO1	SMIM3	RASAL3	SLFN13	NLRX1	FADS1	KRT81	RHOG	RGMB	GPD1L	KRT33A	CHAC1	RNF223
59	FAM20A	FAM160A1	CXCR3	SHFL	CES5A	ELOVL5	KRTAP12-2	PARP2	SYT17	KRT6C	SACM1L	SPTLC2	EPN3
60	CCL18	SEC24D	MCOLN2	SP140L	GPLD1	MGST1	SERPINB7	UQCC2	STRAP	GREB1L	KRTAP1-3	CASP7	SPRR2D
61	LIMA1	ITGA5	MAP4K1	WDFY1	ZMYND8	ACSM3	KRTAP1-1	FAM189B	RHCG	RAN	GPRC5D	TFDP1	SLC25A5
62	SLC4A7	ZNF281	S100B	PLSCR1	ATP1B1	CYP4F8	SFRP1	UPF1	TPI1	LMBRD1	WWOX	LGALS3	SMPD3
63	PHLDB2	OLFML2B	PTPN7	GIMAP4	PPARGC1B	IQCJ	COBLL1	CHERP	DENND4C	MYO9A	LUZP2	SLC26A9	CRCT1
64	FCGR2A	PTTG1IP	ADCY7	PRF1	TPRG1	THRSP	KRTAP11-1	SPHK2	MYO1B	PDCD4	FUT1	NCALD	DYNLL1
65	RUNX1	MME	LRRK1	OAS1	MPZL3	ADTRP	CCL23	SCAMP3	EEF2K	SERPINB3	CRABP2	SERPINB1	CRYBG1
66	CALU	SDR42E1	NFATC2	PARP14	ABCA12	CLPSL2	CTSG	TBL3	SPTSSA	PLCB4	CLPX	TUBA1A	PSORS1C2
67	STEAP4	EMP2	SPOCK2	SETX	SH3BP5L	ZNF726	GALNT1	SGTA	UPP1	SOX5	KRTAP9-7	YWHAQ	APRT
68	ADAMTS5	FAM83F	CRTAM	EPSTI1	IL36B	SC5D	SORCS3	AKNAD1	CRABP2	FNBP1L	SCYGR4	SERPINA12	MAP3K9
69	CAPNS2	LHFPL2	EHF	TNFSF13B	ANKK1	IGFL2	LDLRAD3	WRNIP1	OR2T3	VKORC1L1	PADI3	IL19	CHAC1
70	PMP22	PDPN	LSP1	USP25	TREX2	KRT79	NFKBIZ	PLEKHM1	NANS	ARPC5L	SPRR2F	CAT	CARHSP1
71	MMP1	NRIP3	SPRR2D	CCL5	GLS2	OR4D9	PADI3	GUK1	ADNP	TIMELESS	KRT26	MUC4	FUT1
72	CR1	TRIO	CTSW	TNFSF10	SEMA7A	FASN	TMBIM1	GMEB2	ABCA5	FAM13A	FABP9	LYPD1	HRNR
73	PLAU	PTHLH	WDFY4	PNPT1	GLB1L2	SLCO4C1	CD8B2	ARPC4	P2RX7	SPTBN1	CFAP45	PDZK1IP1	RNF11
74	IL20RA	TMEM119	HLA-DOA	TRIM22	SEMA4A	ACSM6	MASP1	MAP3K11	FAM117B	TPI1	PCSK9	FLG	SLC24A3
75	GTF2I	ZNF697	CD3D	PLAAT4	LCN2	AGPAT3	CCL26	MAP1S	ANXA3	OPHN1	MID1	FGFR1	IL36RN
76	CALCOCO1	ZFYVE16	F5	SPATS2L	HSD17B2	ALDH1L1	LPIN2	CLCN7	PAMR1	PPP4R1	ATP1B3	ELF3	C12orf56
77	TIMP1	GGT6	SEPTIN6	LAG3	MVK	SRD5A1	KRT2	KRT75	NR2C2	CFAP70	KRTAP4-9	SERINC1	PSG7
78	GPLD1	TGFBR1	TBC1D10C	DYNLT1	AP1M2	PM20D1	DAPP1	DAZAP1	HSPBAP1	PNP	TPP2	PDK3	VIPR1
79	TNFRSF11B	ITGB1	ABI3	APOL3	CYP4F2	GK5	KRT39	DNAH17	DLG2	LRP6	IL17A	PRSS27	PDZK1IP1
80	CD93	CTSB	PPM1M	CXCL10	BLMH	CHP1	KRTAP9-4	ACTG1	YWHAQ	SRXN1	CNNM1	ZNF652	GSDMA
81	MMP19	TGFB3	CIITA	CFB	PLA2G2F	GLDC	KRT33B	MECR	GAPDH	PFN1	CCDC85C	CCNE1	KLK8
82	TGFBR1	GPC6	IL2RG	IFI44L	KIF13A	ZP1	KRTAP1-3	UBQLN2	TNFAIP1	RNF180	SCN4B	SERPINB4	FABP5
83	RMND5A	ADAMTS12	IPCEF1	ZC3HAV1	CYB5R2	ALOX15B	GBP1	DDX54	S100A11	ABCA5	CNNM4	FBXW11	SPIRE1
84	DSE	GLIS3	C11orf21	ZCCHC2	KRT23	RTN4	KRTAP26-1	PTPA	BZW1	BMPR1A	ARSF	LRRC55	METTL9
85	UNC13B	CLEC5A	SPRR2B	GBP4	GSDMA	SOAT1	RBMXL1	ZFP41	CANX	MPZL2	IL36G	PRKAR2A	HIGD1A
86	PHLPP1	ADGRE2	INPP5D	APOBEC3G	NSMAF	HEATR4	ALOX15	MYDGF	SHC1	GPR12	KRTAP4-2	ANKRD22	ADIPOR1
87	SRPX	B4GALT1	LTB	XAF1	PREP	METTL7B	NAV3	PGLS	ALDOA	MYBL2	PRRG4	GOT2	TGM6
88	COPS8	SEC31A	VAMP1	CASP10	SRMS	ABHD5	KYNU	TRAF4	LRP4	SUN1	TCN1	CGNL1	TMC5
89	THY1	GALNT5	IL12RB1	IFI44	TMEM86A	CDKL2	TAB3	ACAA1	OR2T11	ARHGEF28	ACTBL2	TXNIP	TREX2
90	CD59	NEBL	XCR1	KLHDC7B	VWA3A	PNLIPRP3	AQP3	SYVN1	MED13L	PTPN14	KRTAP12-2	RAB38	NRBF2
91	PAQR7	DOCK4	BATF	CHMP5	FAM102B	PNPLA3	CORO2A	PARP10	KRT6A	PPARGC1A	ALDH2	ATP1B3	CLCN3
92	LBP	CALU	NOL4L	ARHGEF3	CAV2	LDHD	SERP1	CRELD2	FZD5	KANSL1L	USP9X	UPP1	HSD17B10
93	FAM110B	ZNF469	RASSF5	KLRD1	ARHGAP40	OR2F1	TCHHL1	CNOT3	ZNF721	IL4R	DLG3	UBE2G1	KRT80
94	BICC1	ALPK2	ZNF683	ATP10A	SLC35E4	MVD	CCL4	DRAP1	ACADSB	NFIB	KRTAP5-4	KCNT2	SPTSSA
95	SCEL	MMP1	NIBAN1	LGALS9	RNF207	ZNF117	LYN	SELENOO	ARG2	PRKN	CA2	TUBB6	UCHL3

96	TLNRD1	IGF2	CCDC88C	GPBP1	NR3C1	DGAT2	PLPP3	MAP3K5	ATP5MC3	YKT6	AFAP1L2	SLC7A1	COX6A1
97	MAML3	GASK1B	STAT5A	TRIM34	BICDL1	ISOC1	EML1	FHL1	C1QBP	BBS2	HR	SYNE1	ANKRD10
98	PLA2G2A	MFSD6	CYFIP2	GIMAP5	SLC41A1	RGS9BP	FCER2	TASOR2	PLK2	PRR15L	SLC18B1	SETBP1	MACO1
99	MME	C5AR1	NEFL	RNF213	CARD14	TMEM63C	BLZF1	SEC61A1	GATM	ARHGAP12	KRTAP16-1	IL36G	TMPRSS11D
100	HDAC5	P3H1	ADA2	IRF2	DHCR7	GNPAT	NELL2	HPCAL1	WNT2B	S100A11	CLEC3A	SERPINB3	GLTP

	E1	E10	E11	E12	E13	E2	E3	E4	E5	E6	E7	E8	E9
E1	1	0.78660791	0.89997971	0.91143119	0.91119225	0.84968252	0.78350723	0.88523404	0.86855793	0.84268635	0.92180728	0.88292597	0.8200244
E10	0.78660791	1	0.86534968	0.71699541	0.81617431	0.68374785	0.93852358	0.88648251	0.90683203	0.94025078	0.94185364	0.96142967	0.98823823
E11	0.89997971	0.86534968	1	0.94689883	0.99025324	0.72558849	0.86031557	0.87561789	0.98274608	0.93987944	0.955418	0.95512777	0.90334772
E12	0.91143119	0.71699541	0.94689883	1	0.96458408	0.68774567	0.69667934	0.80331803	0.90739155	0.83387477	0.87273994	0.85011677	0.7570507
E13	0.91119225	0.81617431	0.99025324	0.96458408	1	0.72087399	0.8337098	0.8524621	0.96271384	0.91792038	0.93584377	0.93005029	0.85847414
E2	0.84968252	0.68374785	0.72558849	0.68774567	0.72087399	1	0.69345996	0.77568446	0.71269161	0.68598768	0.75586702	0.7474931	0.71514235
E3	0.78350723	0.93852358	0.86031557	0.69667934	0.8337098	0.69345996	1	0.88317415	0.88064384	0.935876	0.9248227	0.94382542	0.95034811
E4	0.88523404	0.88648251	0.87561789	0.80331803	0.8524621	0.77568446	0.88317415	1	0.87790668	0.88424565	0.91745949	0.91670053	0.90035117
E5	0.86855793	0.90683203	0.98274608	0.90739155	0.96271384	0.71269161	0.88064384	0.87790668	1	0.96706803	0.95496522	0.97034484	0.93449941
E6	0.84268635	0.94025078	0.93987944	0.83387477	0.91792038	0.68598768	0.935876	0.88424565	0.96706803	1	0.95649881	0.96734741	0.95193501
E7	0.92180728	0.94185364	0.955418	0.87273994	0.93584377	0.75586702	0.9248227	0.91745949	0.95496522	0.95649881	1	0.98512173	0.96442431
E8	0.88292597	0.96142967	0.95512777	0.85011677	0.93005029	0.7474931	0.94382542	0.91670053	0.97034484	0.96734741	0.98512173	1	0.9784563
E9	0.8200244	0.98823823	0.90334772	0.7570507	0.85847414	0.71514235	0.95034811	0.90035117	0.93449941	0.95193501	0.96442431	0.9784563	1

Germany South	E1	E2	E3	E4	E5	E6	E7	E8	E9	E10	E11	E12	E13
IL23 SR	0	0	0	0	0	0	0	0	0	0	1	4	1
IL23 R	0	0	0	0	1	1	1	0	0	0	1	1	1
IL23 NR	0	0	0	0	1	0	0	1	0	0	1	2	0
IL23 SNR	0	0	0	0	0	0	0	0	0	0	0	0	0
TNF SR	0	0	0	0	0	0	0	0	0	0	1	0	1
TNF R	0	0	0	0	0	0	0	1	0	0	1	1	2
TNF NR	0	0	0	1	0	0	1	0	1	0	2	3	1
TNF SNR	0	0	0	0	0	0	0	0	0	0	0	1	0
IL-17 SR	0	0	0	0	0	0	0	2	1	0	3	1	1
IL-17 R	0	0	0	0	0	0	1	0	0	0	1	1	1
IL-17 NR	0	0	0	0	0	0	0	0	0	0	1	0	0
IL-17 SNR	0	0	0	0	0	0	0	0	0	0	0	3	1
Sum	*0*	*0*	*0*	*1*	*2*	*1*	*3*	*4*	*2*	*0*	*12*	*17*	*9*
Germany North	E1	E2	E3	E4	E5	E6	E7	E8	E9	E10	E11	E12	E13
IL23 SR	0	0	0	0	2	0	0	0	0	0	1	3	0
IL23 R	0	0	0	0	0	0	0	0	0	0	0	1	0
IL23 NR	0	0	0	0	0	0	0	0	0	1	1	2	0
IL23 SNR	0	0	0	0	0	0	0	0	0	0	1	0	0
TNF SR	0	0	0	0	0	0	0	0	0	0	0	0	0
TNF R	0	0	0	0	1	0	0	0	0	0	0	1	0
TNF NR	0	0	0	0	1	0	0	0	0	0	2	0	2
TNF SNR	0	0	0	0	0	0	0	0	0	0	0	0	0
IL-17 SR	0	0	0	0	2	0	0	0	0	0	1	3	1
IL-17 R	0	0	0	0	1	0	0	0	0	0	0	0	1
IL-17 NR	0	0	0	0	0	0	0	0	0	0	1	0	0
IL-17 SNR	0	0	0	0	0	0	0	0	0	0	0	0	0
Sum	*0*	*0*	*0*	*0*	*7*	*0*	*0*	*0*	*0*	*1*	*7*	*10*	*4*
USA East Coast	E1	E2	E3	E4	E5	E6	E7	E8	E9	E10	E11	E12	E13
IL23 R	2	0	0	0	0	0	0	0	0	0	3	15	2
IL23 NR	1	0	0	0	0	0	0	0	0	0	4	3	2
TNF R	0	0	0	0	2	0	0	0	0	0	5	12	2
TNF NR	2	0	0	0	0	0	0	0	0	1	1	7	3
Sum	*5*	*0*	*0*	*0*	*2*	*0*	*0*	*0*	*0*	*1*	*13*	*37*	*9*
USA North	E1	E2	E3	E4	E5	E6	E7	E8	E9	E10	E11	E12	E13
TNFA SR	0	0	0	0	0	0	2	0	0	0	2	0	1
TNFA R	0	0	0	0	3	0	4	0	0	0	0	1	1
TNFA NR	0	0	0	0	3	0	5	0	0	0	7	2	2
TNFA SNR	0	0	0	0	0	1	0	0	0	0	1	2	0
Sum	*0*	*0*	*0*	*0*	*6*	*1*	*11*	*0*	*0*	*0*	*10*	*5*	*4*

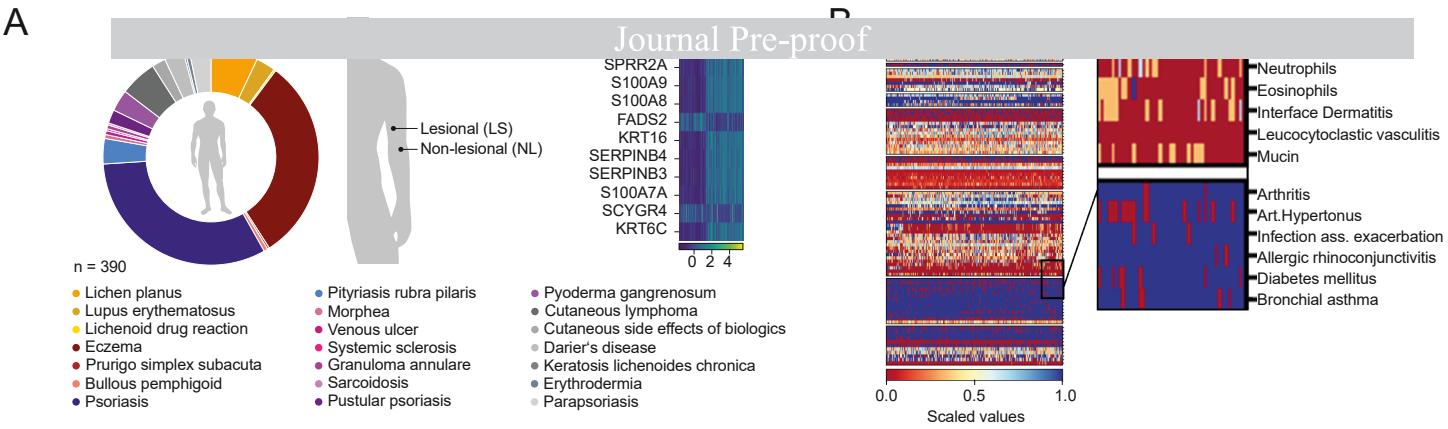

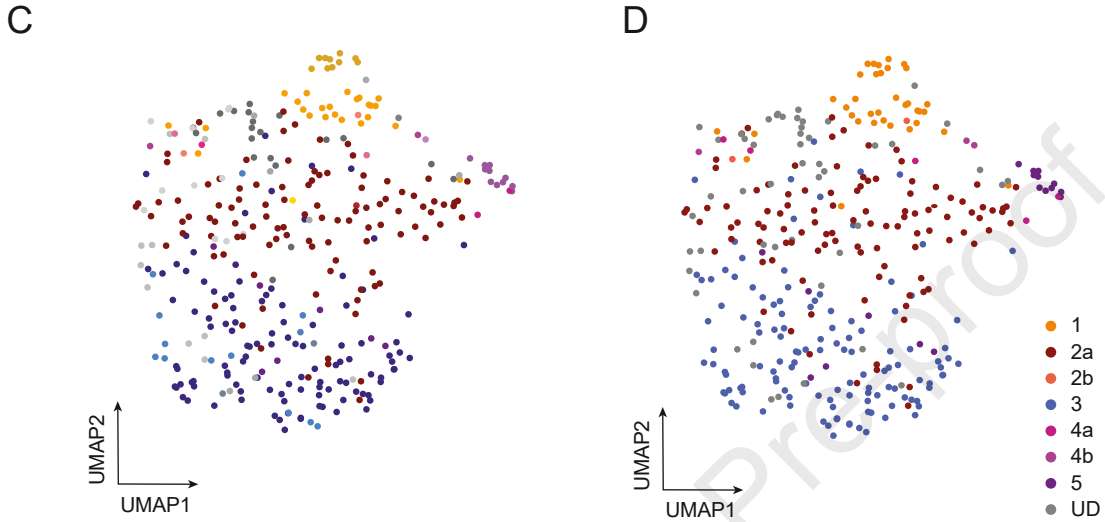

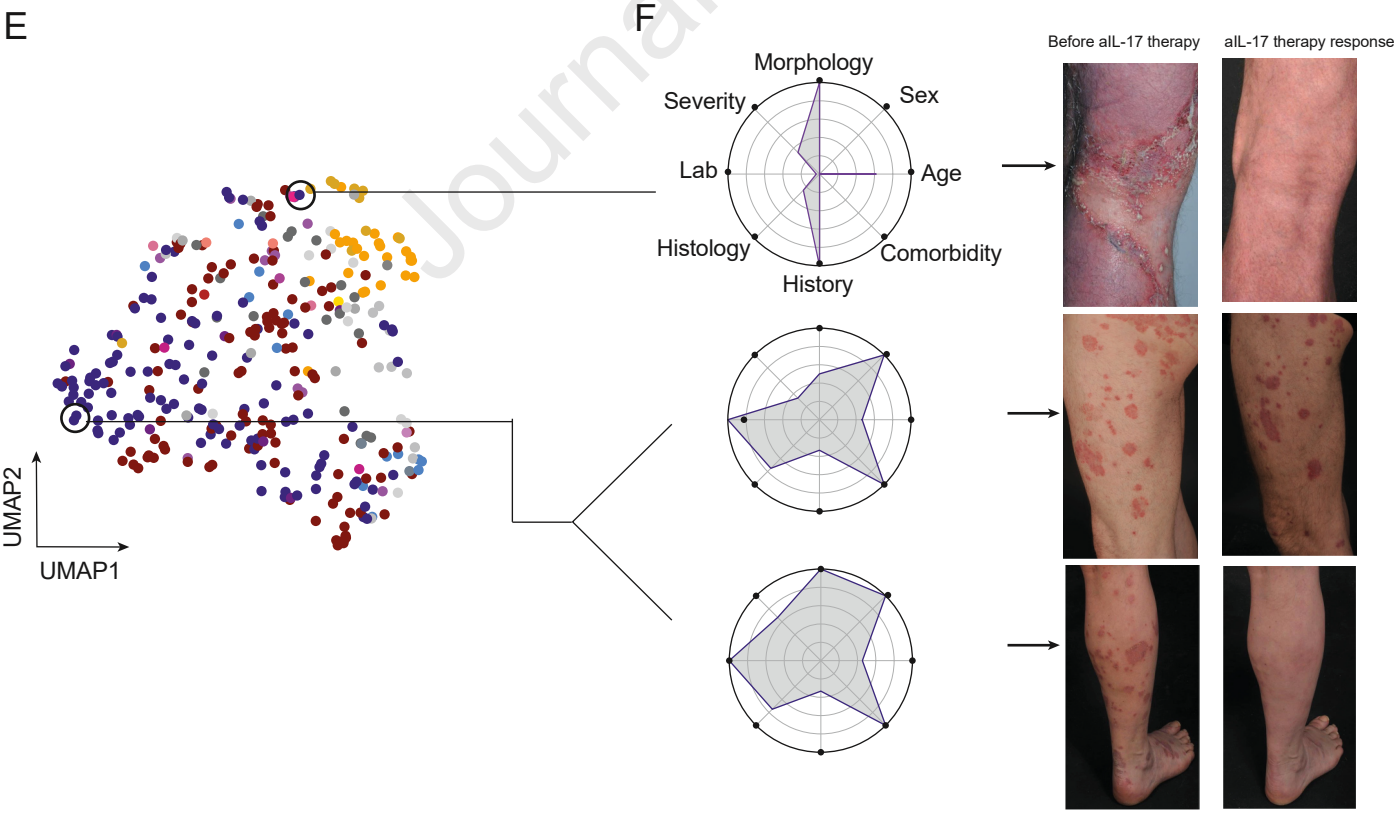

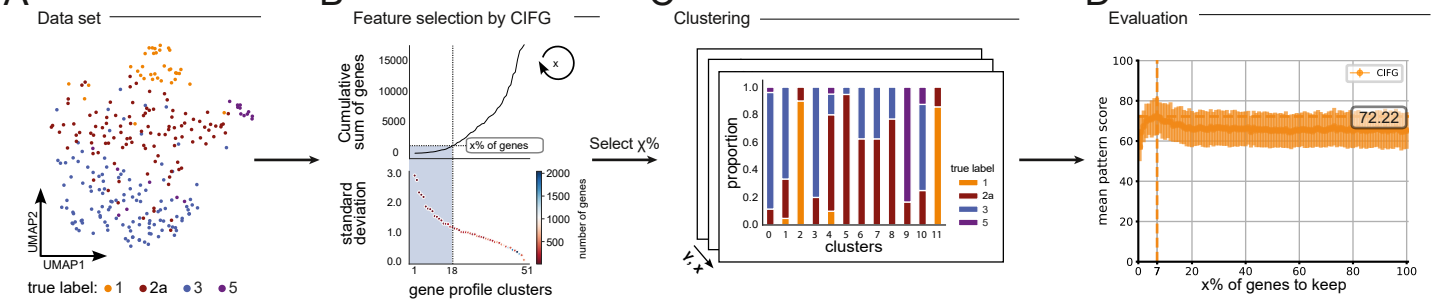

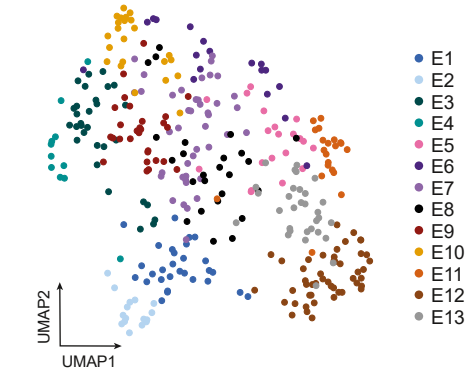

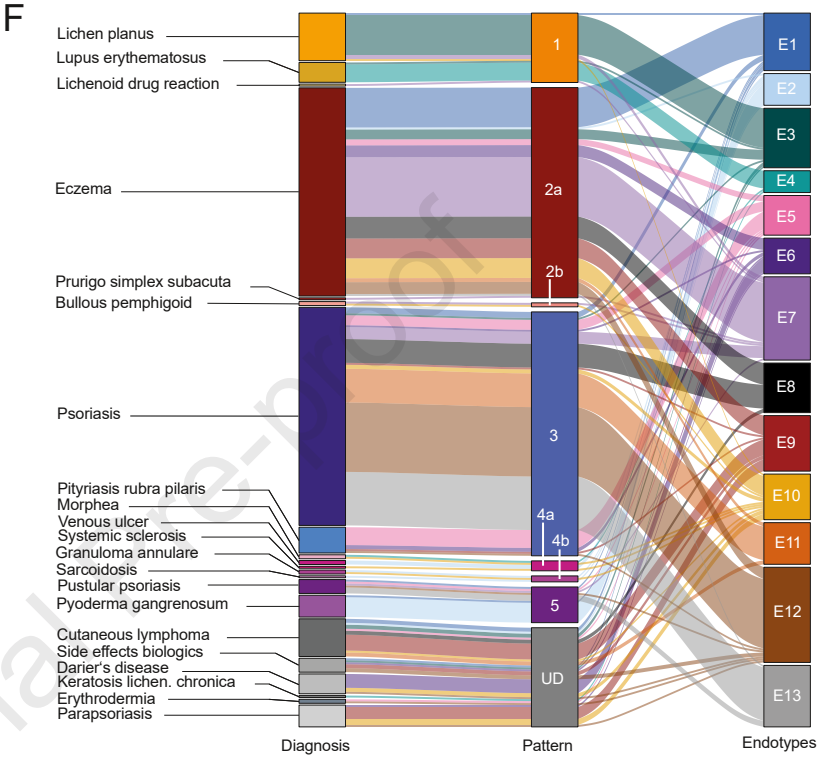

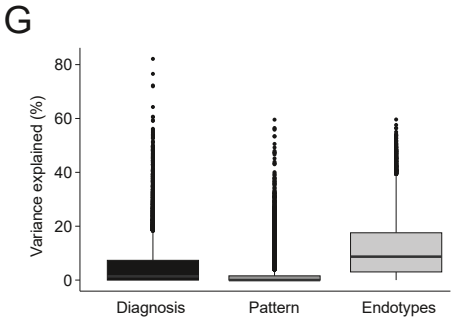

A

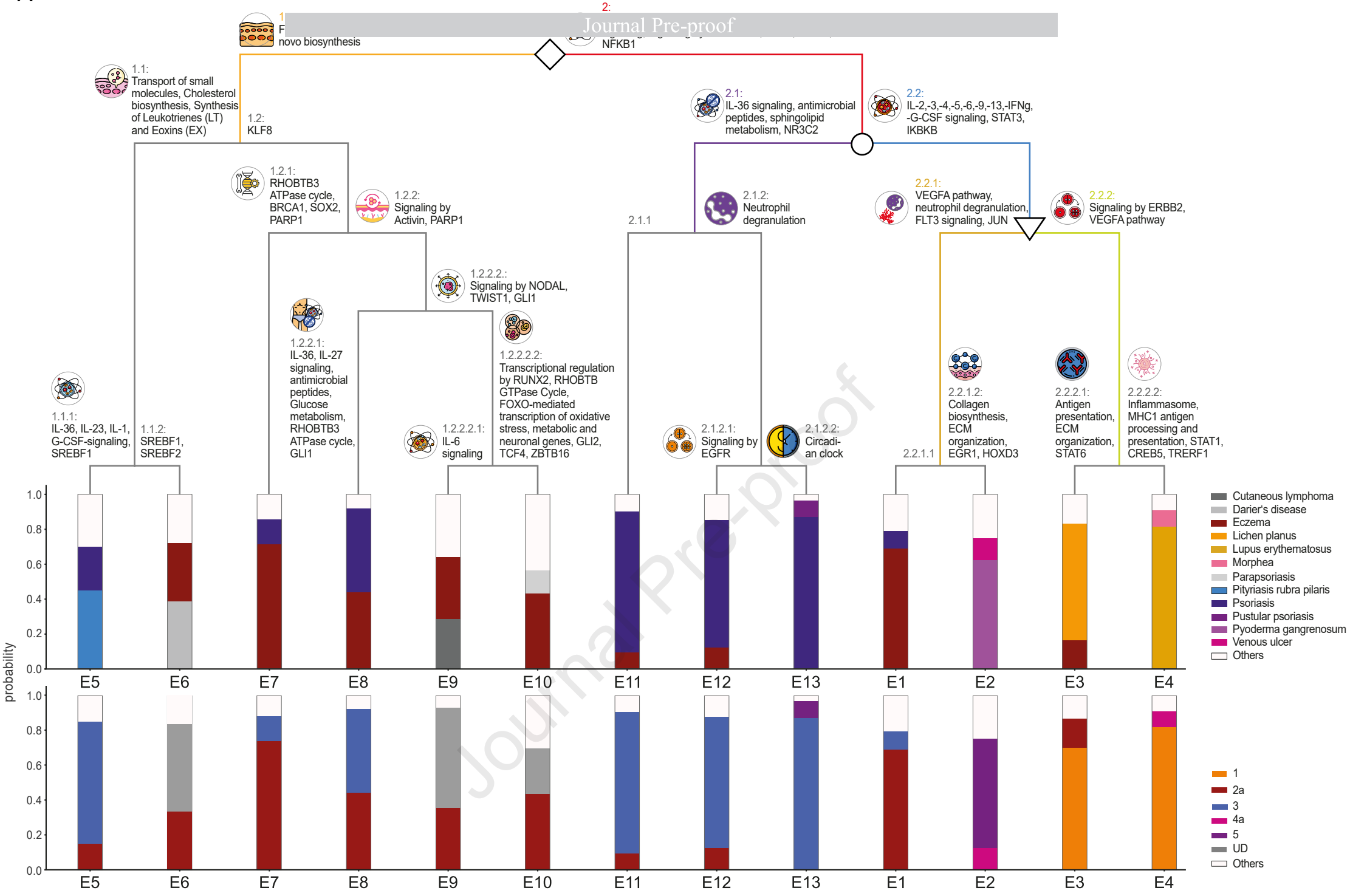

B

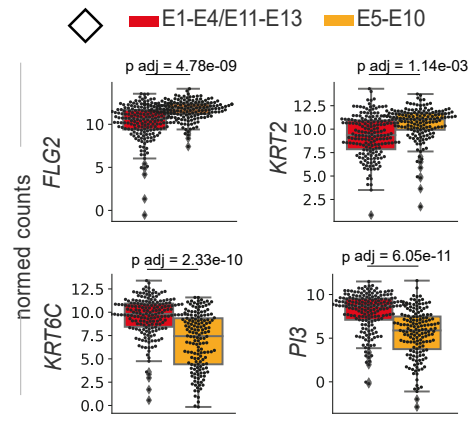

C

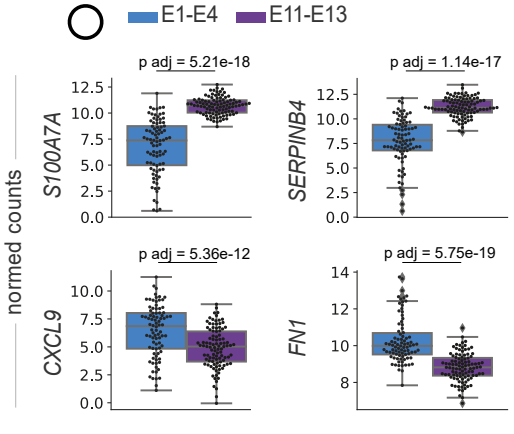

D

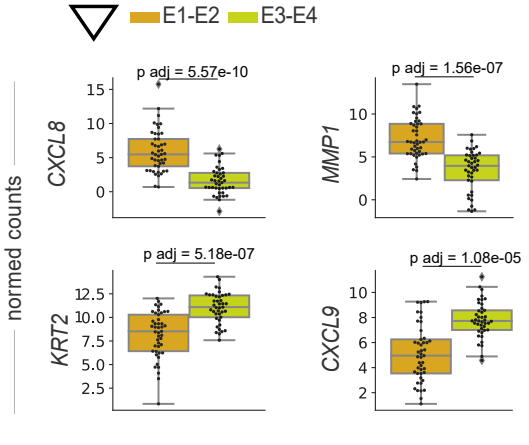

A

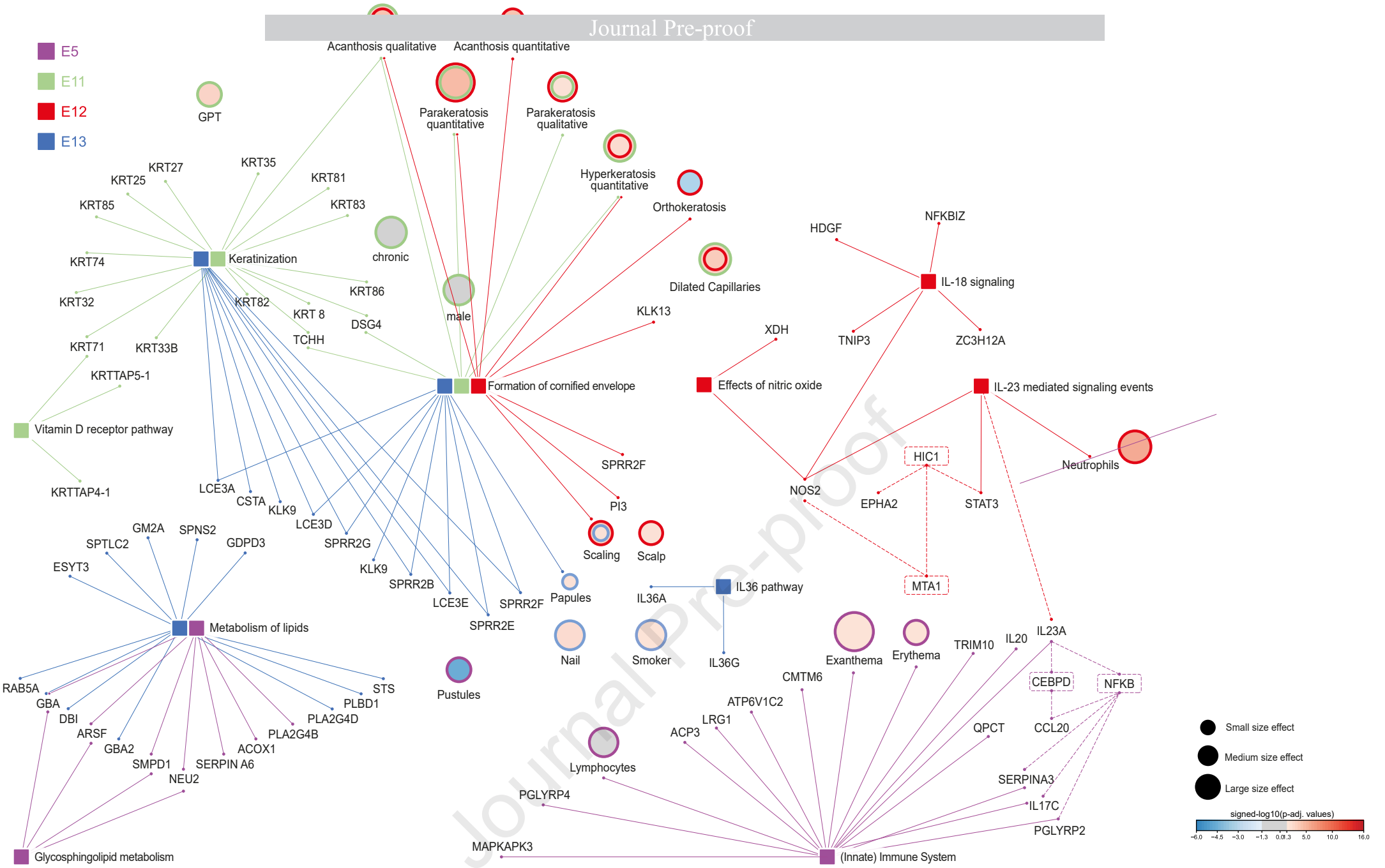

B

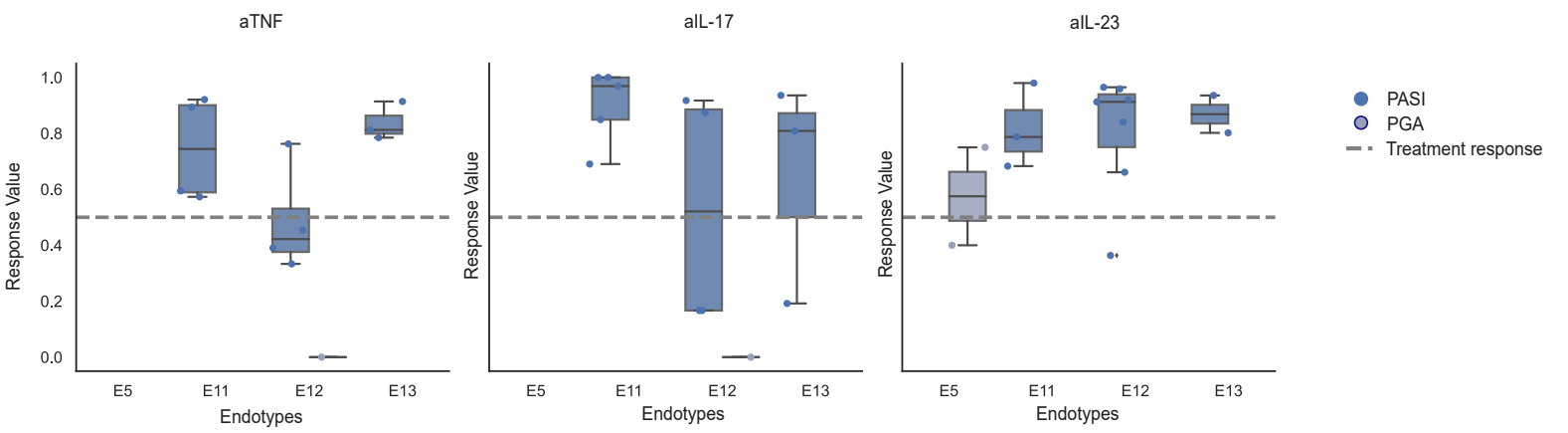

A

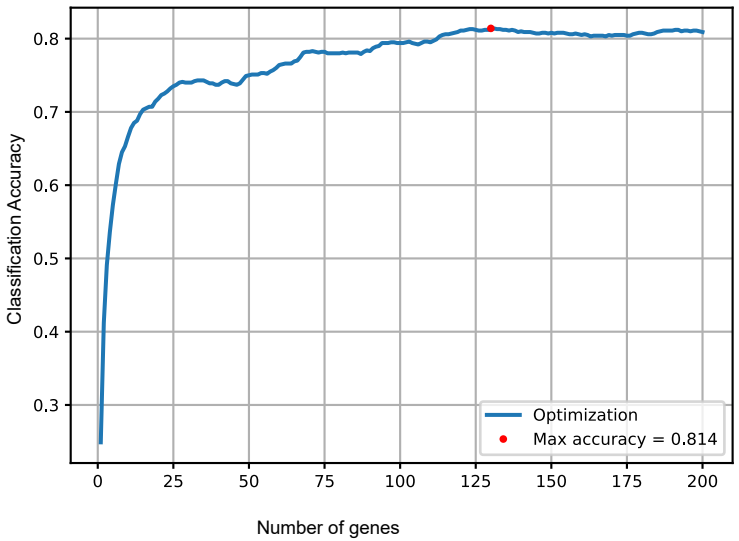

B

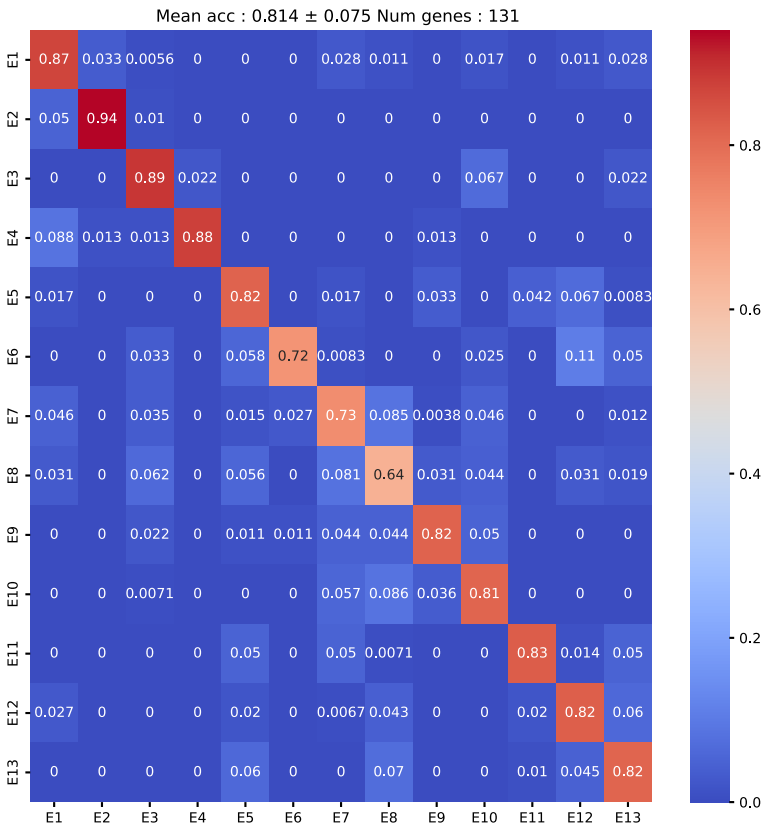

C

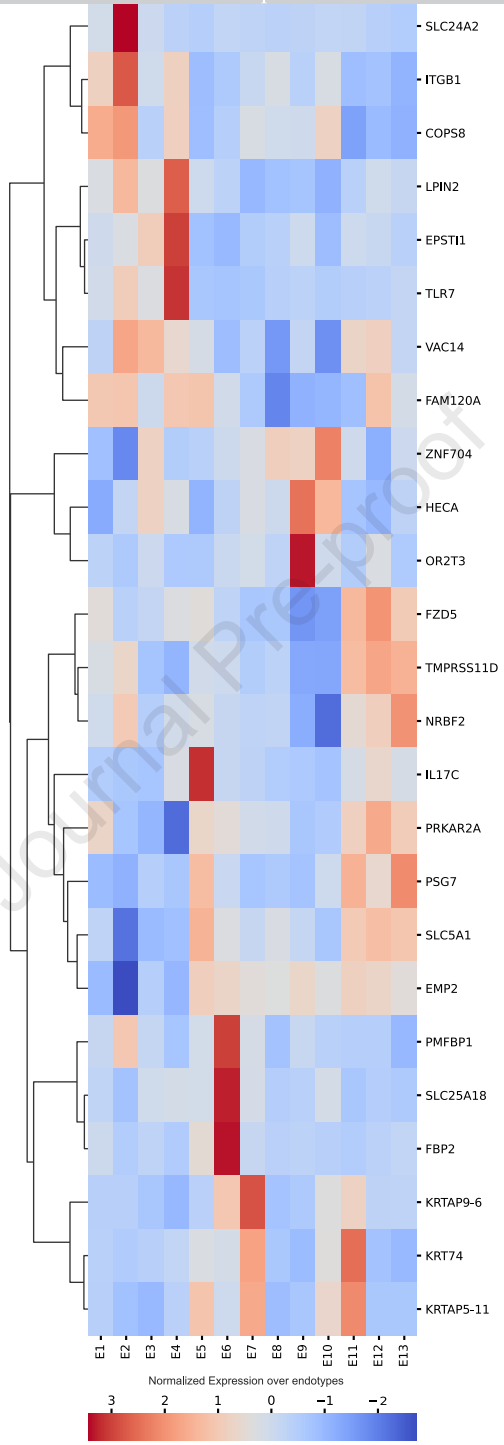

D

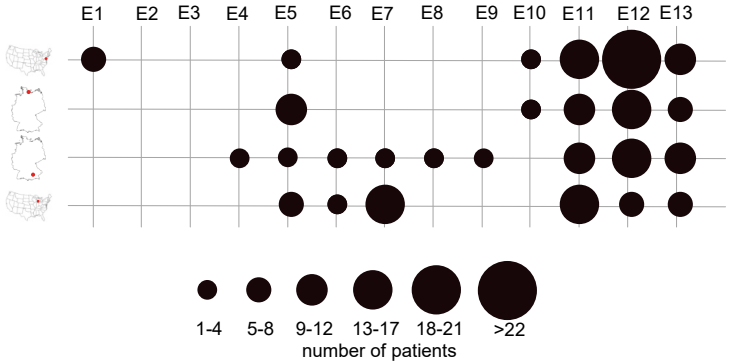

E